ORIGINAL RESEARCH

Atrial Structural Remodeling in Patients With Atrial Fibrillation Is a Diffuse Fibrotic Process: Evidence From High-Density Voltage Mapping and Atrial Biopsy

Takanori Yamaguchi ⬤, MD; Toyokazu Otsubo, MD; Yuya Takahashi, MD; Kana Nakashima, MD; Akira Fukui, MD, PhD; Kei Hirota, MD; Yumi Ishii, MD; Kodai Shinzato, MD; Ryosuke Osako, MD; Mai Tahara, MD; Yuki Kawano, MD; Atsushi Kawaguchi, PhD; Shinichi Aishima, MD, PhD; Naohiko Takahashi, MD, PhD; Koichi Node ⬤, MD, PhD

BACKGROUND: Low-voltage areas (LVAs) in the atria of patients with atrial fibrillation are considered local fibrosis. We hypothesized that voltage reduction in the atria is a diffuse process associated with fibrosis and that the presence of LVAs reflects a global voltage reduction.

METHODS AND RESULTS: We examined 140 patients with atrial fibrillation and 13 patients with a left accessory pathway (controls). High-density bipolar voltage mapping was performed using a grid-mapping catheter during high right atrial pacing. Global left atrial (LA) voltage (V_{GLA}) in the whole LA and regional LA voltage (V_{RLA}) in 6 anatomic regions were evaluated with the mean of the highest voltage at a sampling density of 1 cm^2. Patients with atrial fibrillation were categorized into quartiles by V_{GLA}. LVAs were evaluated at voltage cutoffs of 0.1, 0.5, 1.0, and 1.5 mV. Twenty-eight patients with atrial fibrillation also underwent right atrial septum biopsy, and the fibrosis extent was quantified. Voltage at the biopsy site (V_{biopsy}) was recorded. V_{GLA} results by category were Q1 (<4.2 mV), Q2 (4.2–5.6 mV), Q3 (5.7–7.0 mV), and Q4 (≥7.1 mV). V_{RLA} at any region was reduced as V_{GLA} decreased. V_{GLA} and V_{RLA} did not differ between Q4 and controls. The presence of LVAs increased as V_{GLA} decreased at any voltage cutoff. Biopsies revealed 11±6% fibrosis, which was inversely correlated with both V_{biopsy} and V_{GLA} (r=−0.71 and −0.72, respectively). V_{biopsy} was correlated with V_{GLA} (r=0.82).

CONCLUSIONS: Voltage reduction in the LA is a diffuse process associated with fibrosis. Presence of LVAs reflects diffuse voltage reduction of the LA.

Key Words: atrial fibrillation ■ biopsy ■ catheter ablation ■ fibrosis ■ low-voltage area

Atrial fibrillation (AF) is associated with structural, electrical, and contractile remodeling of the atria. The hallmark of structural remodeling of the atria is fibrosis.[1] Atrial fibrosis produces the substrate to promote AF by interrupting fiber bundle continuity, causing local conduction disturbances, and promoting non-uniform anisotropic conduction.[2] Atrial fibrosis has been histologically identified in patients with AF.[3–6]

Recently, left atrial (LA) bipolar voltage mapping has been widely used during catheter ablation procedures for AF to define the AF substrate. Modern electroanatomical mapping during AF ablation can acquire up to thousands of bipolar voltage points to be projected onto a 3-D geometric model of the atrial endocardium. Low-voltage areas (LVAs), defined as an area with bipolar voltage of less than a specified cutoff (eg,

CLINICAL PERSPECTIVE

What Is New?

- Low-voltage areas (LVAs) in the atria measured during catheter ablation for atrial fibrillation have been considered as a surrogate of local fibrosis without histological validation; numerous studies have been reported based on the premise that local LVA represents local fibrosis.
- However, the present study showed that voltage reduction in the atria of patients with atrial fibrillation was a diffuse process and that the presence of LVAs reflected not only local but also global voltage reduction.
- Right atrial septum biopsy revealed that voltage reduction in the atria was associated with the extent of histological fibrosis.

What Are the Clinical Implications?

- The clinical significance of these findings is that the presence of LVA in the left atrium, evaluated by voltage mapping, is a surrogate for advanced diffuse structural remodeling, that is, diffuse fibrotic remodeling, depending on the voltage cutoff and its extent.
- Given the finding that fibrotic remodeling of the atria is a diffuse process, ablation strategies targeting areas that have been considered local fibrosis, for example, LVA, may not be reasonable.
- Right atrial septum biopsy under the guidance of intracardiac echocardiography and fluoroscopy is a feasible technique to evaluate the histological characteristics of the atria.

Nonstandard Abbreviations and Acronyms

AT	atrial tachycardia
CMC	circular mapping catheter
CSp	coronary sinus pacing
FO	fossa ovalis
GMC	grid mapping catheter
HRAp	high right atrial pacing
ICE	intracardiac echocardiography
LAMRT	left atrial macroreentrant tachycardia
LVA	low-voltage area
V_{biopsy}	voltage at the biopsy site
V_{FO}	voltage of fossa ovalis
V_{GLA}	global left atrial voltage
V_{RLA}	regional left atrial voltage

<0.5 mV), have commonly been considered as a surrogate of the presence of native local fibrotic tissue.[7–11] Clinical data have shown that the presence as well as extent of LVAs is a powerful predictor of arrhythmia recurrence after AF ablation,[9–11] suggesting that fibrosis expressed as LVAs plays an important role in maintaining AF. Numerous studies have described approaches for targeting LVAs as AF substrate modification to reduce recurrence after AF ablation, based on the assumption that local LVA represents local fibrosis.[12–17]

Late gadolinium enhancement-magnetic resonance imaging (LGE-MRI) studies have also suggested that fibrosis is a heterogenous process.[18] However, from a histological perspective in post-mortem material, the extent of fibrosis did not differ among different locations in the atria, suggesting that fibrosis progression is a diffuse process.[6] This discrepancy motivated us to electrophysiologically reassess the characteristics of endocardial bipolar voltage and LVAs in the atria, and to histologically validate the relationship between voltage reduction and fibrosis, which has never been reported. The aim of this study was to evaluate atrial structural remodeling in patients undergoing AF catheter ablation using high-density voltage mapping and endocardial biopsy from the right atrial (RA) septum.

METHODS

Anonymized patient data that support the findings of this study are available from the corresponding author upon reasonable request. The data are not publicly available because it contains information that could compromise the privacy or consent of the study participants.

Study Design and Patient Population

This study consisted of an AF group including 140 patients undergoing AF ablation and a control group including 13 patients with a left accessory pathway. All patients were Japanese. The AF group consisted of 2 groups including a non-biopsy group (n=112) and a biopsy group (n=28). For the non-biopsy group, 189 consecutive patients were initially included using the following inclusion criteria: (1) radiofrequency ablation for non-valvular AF performed between October 2018 and December 2019 in Saga University Hospital; (2) high-density bipolar voltage mapping of the LA during high RA pacing (HRAp) using a grid-mapping catheter (GMC) with a 4×4 electrode configuration (Advisor HD Grid mapping catheter; Abbott). Then, a total of 77 patients were excluded using the following criteria: (1) severe valvular disease (n=1); (2) history of open-heart surgery (n=2); (3) previous ablation in the LA (n=25); (4) hemodialysis (n=2); (5) definitive diagnosis of cardiac amyloidosis before the ablation procedure (n=1); (6) failure to

complete voltage mapping prior to any radiofrequency energy application (n=35); and (7) insufficient mapping density with 5 mm interpolation (n=11). Those patients were excluded after the catheter procedures. The biopsy group was collected from HEAL-AF (Histological Evaluation of Atrial Fibrillation Substrate Based on Atrial Septum Biopsy, Japanese UMIN Clinical Trial Registration UMIN000040781), which is an ongoing observational study conducted in Saga University and Oita University Hospitals to evaluate outcomes after AF ablation based on the histology of RA septum biopsy samples. A total of 69 consecutive patients undergoing biopsy were initially included from this study using the following inclusion criteria: (1) radiofrequency ablation for non-valvular AF; (2) high-density voltage mapping of the LA during HRAp using GMC. Then, 41 patients were excluded using the following exclusion criteria: (1) history of open-heart surgery (n=0); (2) previous ablation in the LA (n=14), (3) hemodialysis (n=0); (4) definitive diagnosis of cardiac amyloidosis before the ablation procedure (n=1); (5) failure to complete voltage mapping and biopsy prior to any radiofrequency energy application (n=7); (6) insufficient mapping density with 5-mm interpolation (n=0); (7) amyloid deposition identified in the atrial biopsy samples (n=3); and (8) samples of insufficient quality for histological evaluation (n=16). Those patients were excluded after the catheter procedures. Then, the remaining 28 patients were examined in the biopsy group. Finally, the AF group consisted of a total of 140 patients. The control group included 13 patients who had no history of AF or any cardiovascular diseases and underwent left accessory pathway ablation via trans-septal approach and high-density voltage mapping of the LA during HRAp using GMC. These studies were approved by the Ethics Committee of Saga University Hospital (reference number, 20190201 for the non-biopsy group; 20200101 for the biopsy group; 20200501 for the control group). All patients gave written informed consent to participate in these studies. The research conformed to the principles outlined in the Declaration of Helsinki.

Transthoracic echocardiography was performed prior to ablation. LA volume was evaluated before ablation by a contrast-enhanced CT scan.[14] Antiarrhythmic drugs, with the exception of amiodarone, were discontinued for at least 5 half-lives before the ablation. Paroxysmal AF was defined as AF that terminates spontaneously or with intervention within 7 days of onset, and non-paroxysmal AF was defined as continuous AF that is sustained beyond 7 days.

High-Density Bipolar Voltage Mapping

Electrophysiological studies and catheter ablation were performed under general anesthesia for the AF group and conscious sedation for the control group. LA geometry and a high-density bipolar voltage map

were created during HRAp at 100 beats per minute (bpm) using a 3D-electroanatomical mapping system (EnSite Precision; Abbott), and a GMC in both the AF group and the control group. Bipolar voltage was defined as the peak-to-peak electrogram amplitude. All bipolar signals, both along and across the splines of the GMC, were collected, and the highest amplitude bipolar signal among signals within a vicinity of <1 mm^2 was displayed on the voltage map.[19] This algorithm minimizes the directional sensitivity, which describes the influence of the angle of incidence between the propagating wavefront and the electrode pair on the bipolar electrogram morphology.[20] Any premature atrial beats were strictly excluded. The maximum distance between the mapping points (interpolation) was set at 5 mm. The internal projection of the geometry's electrical information was also set at 5 mm. Bipolar electrograms were filtered by a bandpass to frequencies between 30 and 500 Hz. The GMC was manipulated through an Agilis sheath (Abbott) to prevent insufficient contact with the atrial wall, and the LA atrial septum was also carefully mapped by looping the sheath and GMC. In a subset of 35 patients from the non-biopsy group, a high-density voltage map of the LA was also created during coronary sinus pacing (CSp) at 100 bpm to compare bipolar voltage between HRAp and CSp. In another subset of 20 patients from the non-biopsy group, a high-density voltage map of the LA was also created during HRAp at 100 bmp using a 20-pole circular mapping catheter (CMC) with a 1-mm electrode length and 2-mm interelectrode spacing (ReflectionHD; Abbott) to compare the bipolar voltage between GMC and CMC. In the biopsy group, a high-density bipolar voltage map of the RA septum was also created. The location of the biopsy site and fossa ovalis (FO) was confirmed by intracardiac echocardiography (ViewFlex; Abbott) and annotated with the GMC on the geometry. Patients with AF at the beginning of the procedure had an external or internal biphasic direct current cardioversion (DC) to restore sinus rhythm. When DC up to 270 J failed to restore sinus rhythm (SR) or SR could not be maintained due to frequent AF recurrence before any RF application, those patients were excluded to avoid any impact of RF ablation on the voltage maps, as mentioned above.

Catheter Ablation and Induction of Atrial Tachycardia

PVI was performed in all patients using a contact force sensing catheter (TactiCath Quartz; Abbott). After the PVI, atrial burst pacing from coronary sinus until 2:1 atrial capture was performed to induce LA macroreentrant tachycardia (LAMRT) and cavotricuspid isthmus-dependent atrial flutter before and after bolus injection of 10 µg isoproterenol. An LAMRT was defined as a

cycle length of >180 ms that lasted >5 minutes, and the reentrant circuit was confirmed by electroanatomical mapping and/or post-pacing interval mapping in the LA. Critical isthmus was defined as the narrowest isthmus and the most crowded isochronal zone on the activation map.

Analysis of Voltage Map

Voltage maps and activation maps were analyzed offline. The following regions were excluded from the analysis of LA: LA appendage (LAA); LA ridge between PV and LAA; PVs at the antral region; mitral annual region, defined as a region within 10 mm of the atrial side from the minimum atrial electrogram recording site. In order to further minimize the influence of directional sensitivity, the LA surface was subdivided into an area of 1 cm^2, and the highest voltage in each 1 cm^2 was manually acquired (Figure 1). The distance between the acquired points was set to be at least 5 mm. Global LA voltage (V_{GLA}) was measured as the mean of the highest voltages in each 1 cm^2 area in the whole LA (1 cm^2-area method). Regional LA voltage (V_{RLA}) according to 6 anatomical regions (anterior, septum, roof, inferior, posterior, and lateral) was also evaluated as the mean of the highest voltage in each 1 cm^2. The method of subdividing the LA into 6 regions and the assessment of intra- and inter-observer variability are described in Data S1 and S2. The relative V_{RLA} of each anatomical region was calculated by the following formula: relative $V_{RLA}=100 \times V_{RLA}/$mean V_{RLA} of Q4. The extent of LVAs in the LA was evaluated at the cutoff of <0.1 mV ($LVA_{0.1}$), <0.5 ($LVA_{0.5}$), 1.0 ($LVA_{1.0}$), and 1.5 ($LVA_{1.5}$), and an LVA was defined as a total area of >0.5 cm^2 for $LVA_{0.1}$ and >3.0 cm^2 for the other cutoffs. V_{GLA} during CS pacing (CSp) at 100 bpm was also evaluated in the subset of 35 patients of the non-biopsy group. To exclude the influence of pacing stimuli on the voltage, inferior and lateral regions were excluded from this analysis. V_{GLA} by CMC during HRAp at 100 bpm was also evaluated in the subset of 20 patients in the non-biopsy group. In patients with $LVA_{0.5}$, the relationship between voltage cutoffs and extent of the LVAs at each cutoff was evaluated. In this analysis,
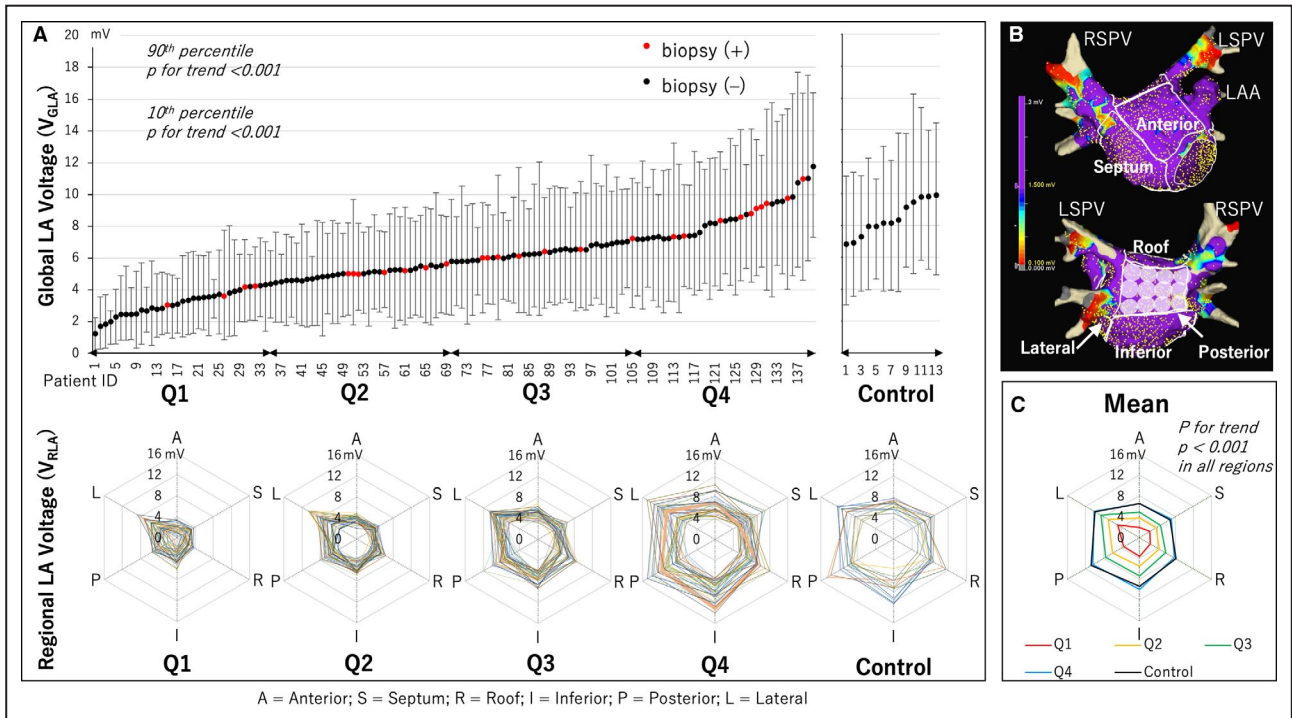

Figure 1. Distribution of global and regional LA voltage.
A, Distribution of the global LA voltage (V_{GLA}) ordered from lowest to highest in the AF group and the control group. The range bar corresponds to 10th and 90th percentiles of voltage of each patient. Q1 to Q4 show quartiles of the AF group based on V_{GLA}. Red dot shows a patient with atrial biopsy, while black dot shows a patient without biopsy. The radar charts show the mean voltage value of the 6 anatomical regions of the LA (V_{RLA}) (A, anterior; S, septum; R, roof; I, inferior; P, posterior; L, lateral) for all patients in each quartile and the control group. **B**, LA was divided into the 6 anatomical regions to calculate each V_{RLA}. The white tags on the posterior wall were 1 cm in diameter. The maximum voltage in each 1 cm^2 area was selected with reference to these tags, and the V_{GLA} and V_{RLA} at each anatomical region were calculated as the mean of these values. **C**, The radar chart shows the mean V_{RLA} for each quartile and the control group. V_{RLA} decreased in all regions as the quartile moved down. The V_{RLA} of Q4 and the control was similar in all regions. AF indicates atrial fibrillation; LA, left atrium; LAA, left atrial appendage; LSPV, left superior pulmonary vein; and RSPV, right superior pulmonary vein.

the extent of LVAs at the cutoffs of <0.75 and <1.25 mV was additionally evaluated.

Validation of the 1 cm^2-Area Method for the Evaluation of V_{GLA} and V_{RLA}

We evaluated V_{GLA} and V_{RLA} using all appropriately annotated points (all-annotated-point method) in a subset of 25 randomly selected patients consisting of 5 patients selected from each quartile and the control group. In the all-annotated-point method, the geometry of each LA region and all the voltage data annotated on the surface of each were extracted from the intraoperative recordings in csv file format, and the V_{RLA} for each LA region was calculated. Similarly, the geometry of the whole LA excluding the PVs and LAA was determined, and V_{GLA} was calculated using all the voltage data on the geometry. V_{GLA} and V_{RLA} were then compared using those 2 methods.

Atrial Septum Biopsy

Atrial septum biopsy was additionally performed before any RF applications in the biopsy group. A bioptome (104 cm with a 2.46 mm^3 tip; Cordis, Miami Lakes, FL) was directly advanced to the atrial septum through the steerable sheath. Using intracardiac echocardiography (ICE, ViewFlex; Abbott) as well as fluoroscopy, biopsy was performed at the posterior portion of the limbus of FO. At the biopsy site, which was annotated on the 3D geometry using the GMC, we selected the 6 highest voltages within the area (13×13 mm) and calculated the mean as V_{biopsy}. At the biopsy site, the presence of a slow conduction zone, defined as <27 cm/s,[21] was also assessed by an isochronal activation map created during HRAp. Three samples with 1 to 3 mm sample size were successfully obtained in all patients, which were fixed in 4% paraformaldehyde and embedded in paraffin for histological evaluation. The tissues were sliced with 5 μm thickness and deparaffinized sections were stained with Masson's trichrome and Congo Red. Patients in whom amyloid deposition was identified were excluded, as mentioned above. Each slide stained with Masson's trichrome was digitally scanned using a digital slide scanner (NanoZoomer S60, Hamamatsu, Japan). Using an image analysis platform (HALO, Indica Labs, Corrales, NM), the edge of the myocardial tissue was manually annotated, excluding the endocardial connective tissue and adipose tissue. The percentage of the area with atrial fibrosis (%fibrosis), including perivascular and interstitial fibrosis, was quantitatively estimated using the HALO area quantification algorithm. Sufficient quality of biopsy samples for histological evaluation was defined as including >0.2 mm^2 of myocardial tissue excluding the endocardial connective tissue and adipose tissue. Two independent observers who were blind to the patients'

clinical information analyzed the samples, and the mean value of %fibrosis was determined. The samples were reviewed by a pathologist.

Analysis of the Voltage of FO

We also analyzed the voltage of FO (V_{FO}) adjacent to the biopsy site. During voltage mapping of the RA septum, the location of the FO was also confirmed by ICE and annotated on the voltage map. FO was equally divided into 4 parts and the highest voltage in each part was recorded, and V_{FO} was calculated as the mean of the 4 highest voltages.

Statistical Analysis

For the goodness-of-fit test for normality, the Shapiro-Wilk test was used when the sample size was <2000, and the Kolmogorov-Smirnov Lillefors test was used when the sample size was ≥2000. Normally distributed data were expressed as the mean±standard deviation (SD), and non-normally distributed data as the median and interquartile range (IQR). Continuous data were analyzed using the unpaired t test for normally distributed data, and the Wilcoxon rank sum test for non-normally distributed data. Categorical data were analyzed using the Chi-squared test or Fisher's exact test, as appropriate. Patients in the AF group were ordered from the lowest to the highest based on V_{GLA}, and classified into quartiles (Q1–Q4) (Figure 1). In addition, range bars corresponding to 10th and 90th percentiles of the voltage for each patient were shown in the figure. Patients in the control group were also ordered from the lowest V_{GLA} to the highest V_{GLA}, and compared with Q4 of the AF group. Baseline characteristics and electrophysiological data were compared across the quartiles using trend tests, in which the Spearman's rank correlation coefficient and the Cochran-Armitage test were used for continuous and categorical data, respectively. The Spearman's rank correlation coefficient was also used to evaluate trends for 10th and 90th percentile voltage of each patient. Simple and multiple linear regression analyses were performed to evaluate demographic and clinical factors associated with V_{GLA} in the AF group. Subsequently, multiple logistic regression analyses adjusted for the demographic and clinical factors significantly associated with V_{GLA} were performed to evaluate the relationship between presence of LVA and V_{GLA}. The extents of $LVA_{0.1}$, $LVA_{0.5}$, $LVA_{1.0}$, and $LVA_{1.5}$ were compared to V_{GLA} using a scatterplot. Since the LVAs appeared as V_{GLA} decreased below some thresholds, linear regression analyses between V_{GLA} and LVA extent were performed in patients who had V_{GLA} below the threshold. Each threshold was determined by a receiver operating characteristic (ROC) curve. In patients with $LVA_{0.5}$ identified, the relationship between LVA size and each voltage cutoff value (0.5, 0.75, 1.0, 1.25, and 1.5 mV) was evaluated by the linear mixed effects model,

considering repeated measurements for each patient. In each quartile (Q1–Q4), V_{RLA} was compared in an order of anterior, septum, roof, inferior, posterior, and lateral wall using the Spearman's rank correlation coefficient. For a comparison of the relative V_{RLA} in the 6 anatomical regions, the one-way analysis of variance (ANOVA) test was used. In addition, the prevalence of LVA in each anatomical region at each voltage cutoff was compared in the same order using the Cochran-Armitage test. Intra- and inter-observer agreement was tested with intraclass correlation coefficient (ICC) score. A P-value of <0.05 was considered statistically significant. JMP pro software (version 14.2, SAS Institute Inc., Cary, NC, USA) was used for the analysis.

RESULTS

Patient Characteristics

V_{GLA} results by category were Q1 (<4.2 mV), Q2 (4.2–5.6 mV), Q3 (5.7–7.0 mV), and Q4 (≥7.1 mV). Baseline characteristics and electrophysiological data across the quartiles of V_{GLA} in the AF group and those of the control group are shown in Table. In the AF group, as the quartiles moved down, patients were older, more female, and more frequently had non-paroxysmal AF type, a history of congestive heart failure, higher CHA_2DS_2-VASc scores, lower renal function, lower left ventricular ejection fraction, and larger LA size. Simple and multiple linear regression analyses in the AF group revealed that age, female sex, non-paroxysmal AF type, and LA volume were significantly associated with V_{GLA} (Table S1). Voltage maps were created using 2549±811 acquired points during HRAp in the AF group. A total of 78±20 were used to calculate V_{GLA} by the 1 cm²-area method for each patient in the AF group. The number of points of maximum voltage obtained in each LA region in the AF group was 17±5 in the anterior, 15±6 in the septum, 6±3 in the roof, 20±6 in the inferior, 13±5 in the posterior, and 7±3 in the lateral. In the control group, a total of 2, 132±412 were acquired and 72±14 highest voltage values were used to calculate the V_{GLA} by the 1 cm²-area method. The number of points of maximum voltage obtained in each region in the control group was 15±3 in the anterior, 15±5 in the septum, 6±2 in the roof, 14±5 in the inferior, 13±3 in the posterior, and 7±2 in the lateral. The V_{GLA} and V_{RLA} evaluated by the 1 cm²-area method showed strong positive correlations with those evaluated by the all-annotated-point method (r=0.974, P<0.001 for V_{GLA}, r=0.748–0.923, P<0.001 for V_{RLA}) (Figures S1 and S2).

Distribution of V_{GLA} and V_{RLA}

V_{GLA} was distributed along a continuum rather than a discontinuous curve when ordered from lowest to highest, and both the 10th and 90th percentiles of voltages in each patient decreased as V_{GLA} decreased (Figure 1). The radar charts consisting of V_{RLA} of each anatomical region showed that V_{RLA} at any region decreased as the quartile moved down. There were no significant differences in V_{GLA} and V_{RLA} at any region between Q4 and the control group (Figure 1 and Figure S3). The relative V_{RLA} showed no significant difference between regions in any quartile, when the lateral was excluded from the analysis (Figure S4), showing that the rate of voltage reduction was uniform in each LA region, except for the lateral. Furthermore, V_{RLA} of any region was not only linearly correlated with V_{GLA} but was also correlated between regions (Figure S5 and Table S2).

Distribution of Bipolar Voltage Values

Histograms of all bipolar voltage values in all patients in each quartile and the control group are shown in Figure 2. Histograms of all quartiles showed a non-normal distribution with lower quartiles skewed to the right. However, the unimodal distribution was consistently maintained (Figure 2A). The median value of each patient was positively correlated with V_{GLA} (median=−0.4+1.0×V_{GLA}, r=0.984, Figure S6). Both the density curve and the cumulative probability curve were very similar between Q4 and the control group (Figure 2B).

Relationship Between Presence of LVA and V_{GLA}

The presence of LVAs increased as the quartile moved down at any voltage cutoff (Figure 3A and 3B). $LVA_{0.1}$ was only identified in Q1 (31%), and $LVA_{0.5}$ was only identified in Q1 (49%) and Q2 (3%). Multiple logistic regression analysis adjusted for the 4 variables including age, female sex, non-PAF type, and LA volume, which were significantly associated with V_{GLA}, revealed that V_{GLA} independently predicted the presence of LVA at cutoff values of 0.5, 1.0, and 1.5 mV (eg, for $LVA_{1.0}$, odds ratio 0.42, 95% confidence interval 0.276–0.640 per 1 mV increase) (Table S3). For $LVA_{0.1}$, multivariate logistic regression analysis could not be performed due to the small number of patients with $LVA_{0.1}$ (n=11). The presence of LVAs by region decreased in the order of anterior, septum, roof, inferior, posterior, and lateral at any voltage cutoff (Figure 3C). On the other hand, V_{RLA} increased in the same order at any quartile, and the same trend was observed in the control group (Figure 3D).

Relationship Between V_{GLA} and the Extent of LVA

When V_{GLA} values and LVA extent were plotted on a scatter plot, LVA appeared when V_{GLA} was below a certain threshold value (2.6, 4.0, 5.5, and 7.0 mV, for $LVA_{0.1}$, $LVA_{0.5}$, $LVA_{1.0}$, and $LVA_{1.5}$, respectively,
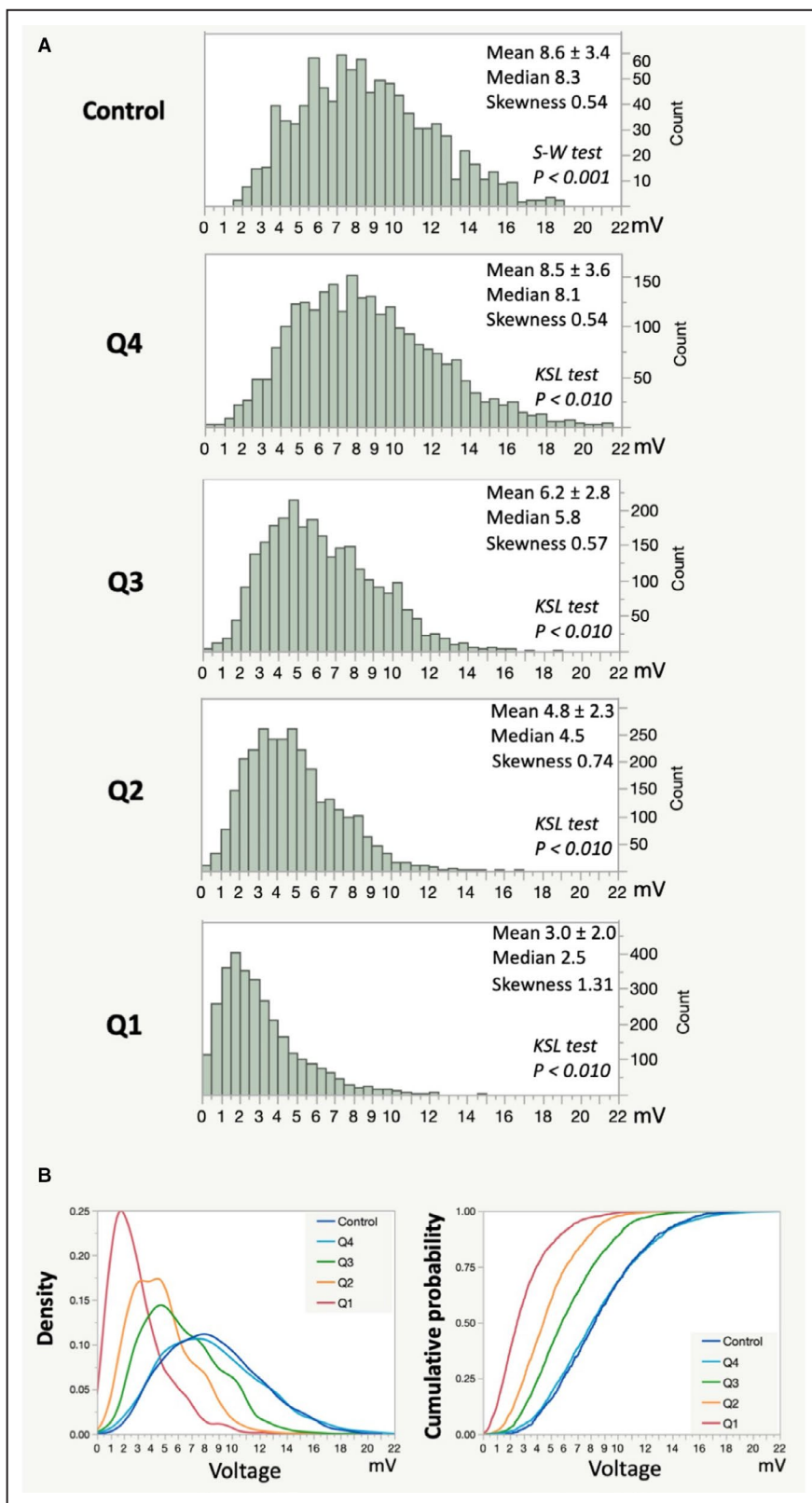
Figure 2. Distribution of bipolar voltage values in all patients in each quartile and the control group.
A, Histograms of all bipolar voltage values in all patients in each quartile and the control group are shown. Each histogram consisted of a total of 2999 (Q1), 2832 (Q2), 2645 (Q3), 2492 (Q4), and 931 (control) voltage values. **B**, A density curve and cumulative probability curve of each quartile and the control group are shown. KSL indicates Kolmogorov-Smirnov Lillefors; and S-W, Shapiro-Wilk.
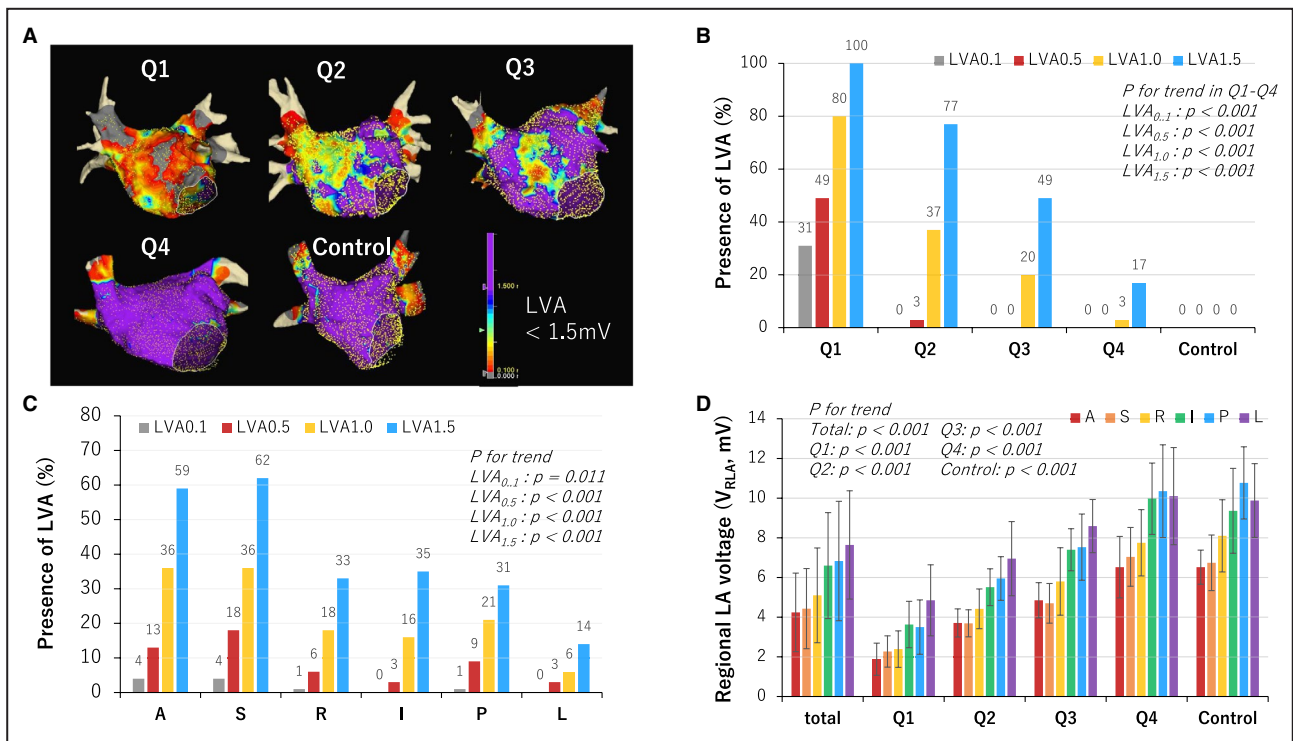
Figure 3. Presence of LVA and regional LA voltage in each quartile and the control group.
A, Examples of voltage map of each quartile and the control group. LVA was defined as <1.5 mV. The color gradation indicates the serial changes in the voltage amplitude from purple at 1.5 mV to grey at 0.1 mV as shown in the color bar at the lower right in the panel. **B**, The presence of LVA by quartile and in the control group at different voltage cutoffs, which increased as the quartile moved down at any voltage cutoff, and as the voltage cutoff increased. No LVAs were identified in the control group even with a voltage cutoff of 1.5 mV. **C**, The presence of LVA by region decreased in the order of anterior, septum, roof, inferior, posterior, and lateral at any voltage cutoff. **D**, Regional LA voltage (V_{RLA}) increased in the same order at any quartile, and the same trend was observed in the control group. LA indicates left atrium; and LVA, low-voltage area.

Figure 4). There was an inverse relationship between V_{GLA} and the LVA extent in patients with V_{GLA} below the threshold. Furthermore, the relationship between voltage cutoffs and the LVA extent was analyzed in patients with $LVA_{0.5}$ identified (n=22). There was a positive linear relationship between LVA extent and voltage cutoffs with a common slope (LVA extent $[cm^2]=LVA_{0.5}+30\times$(voltage cutoff$-0.5$), $R^2=0.94$, $P<0.001$, Figure S7).

Relationship of Global and Regional Voltage Between HRA and CS Pacing

Global LA voltage during CSp (V_{GLA-CS}) was additionally measured in a subset of 35 patients in the AF group. The patient characteristics of this subset are shown in Table S4. There was no significant difference in the number of selected voltage values between HRAp and CSp (51±12 versus 53±9 points per map, $P=0.422$). Although the distribution of LVAs was slightly different, V_{GLA} and V_{GLA-CS} were similar ($V_{GLA-CS}=0.1+1.1\times V_{GLA}$, $r=0.94$, $P<0.001$, Figure S8). V_{RLA} of the LA anterior, septum, and posterior were also similar between HRAp and CSp ($r=0.78-0.92$, Figure S8).

Comparison of V_{GLA} Between GMC and CMC

Voltage maps were created by CMC and 1914±452 points were acquired during HRAp in the subset of 20 patients. A total of 77±26 highest voltage values were used to calculate V_{GLA} by CMC for each patient. There was a strong linear relationship between the 2 mapping catheters ($r=0.979$, $P<0.01$), and V_{GLA} by CMC was $0.75\times V_{GLA}$ by GMC (Figure S9).

Impact of Amiodarone on V_{GLA} and Presence of LVA

Amiodarone was prescribed in 12 patients in the AF group (8 in Q1, one in Q2, 3 in Q3, and none in Q4) and none in the control group. There was no significant difference in patient characteristics, V_{GLA}, V_{RLA}, or the presence of LVA between patients receiving amiodarone (n=8) and those not receiving amiodarone (n=27) in Q1 (Table S5).

Inducibility of LAMRT

All patients successfully completed PVI, and induction of LAMRT was attempted after PVI. A total of
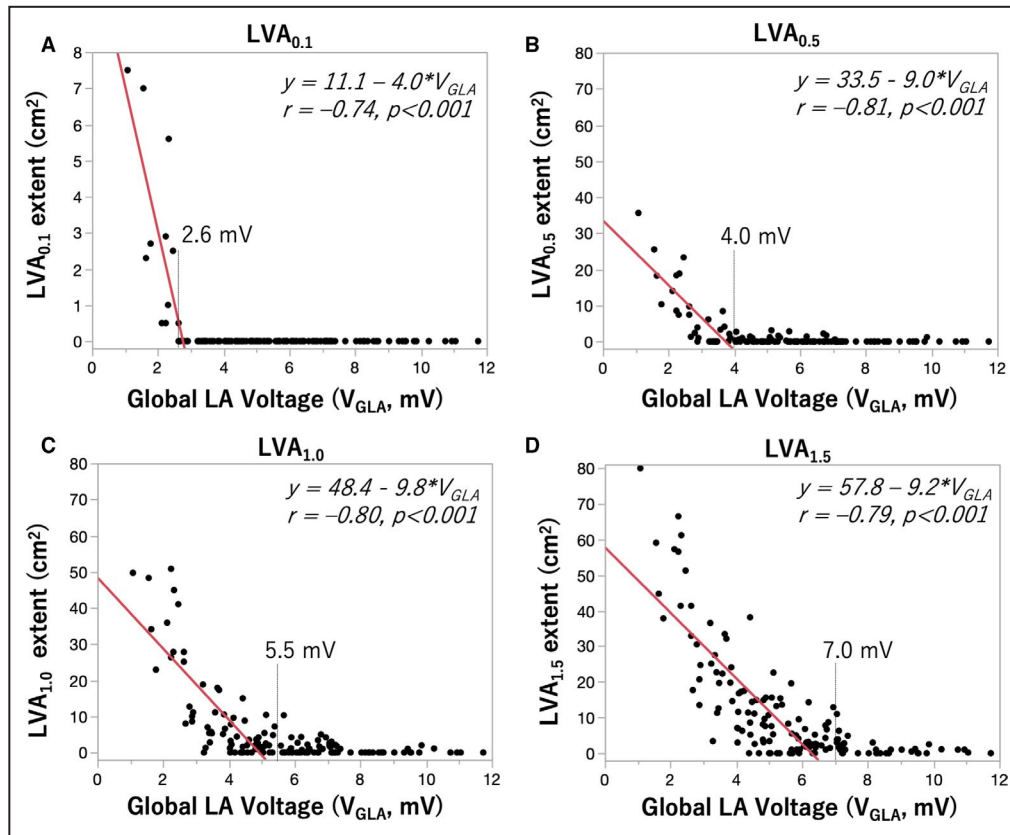
Figure 4. Relationship between global LA voltage and the extent of LVA.
Relationship between global LA voltage (V_{GLA}) and the extent of LVA at different voltage cutoffs (0.1 mV for **A**, 0.5 mV for **B**, 1.0 mV for **C**, 1.5 mV for **D**). Each dot shows data for each patient. LVA appears when V_{GLA} is below a certain threshold value (2.6, 4.0, 5.5, and 7.0 mV, for $LVA_{0.1}$, $LVA_{0.5}$, $LVA_{1.0}$, and $LVA_{1.5}$, respectively). There was an inverse relationship between V_{GLA} and the LVA extent of patients with V_{GLA} below each threshold. LA indicates left atrial; and LVA, low-voltage area.

21 patients (15%) had inducible LAMRTs. Eleven patients had single LAMRT. Ten patients had second LAMRT after elimination of the first LAMRT. Five patients had third LAMRT after elimination of the second LAMRT. The mean cycle lengths (CL) of the first, second, and third LAMRTs were 228±28, 273±45, and 292±53 ms, respectively. In total, 36 LAMRTs were induced: roof reentrant (n=13); perimitral (n=12); AT localized in the anterior (n=5); biatrial tachycardia (n=4); and AT localized in the posterior (n=1) and in the septum (n=1). All of the third LAMRTs were biatrial tachycardia. Examples of LAMRT are shown in Figure S10. Inducibility of LAMRTs increased as the quartile moved down (Q1, 37%; Q2, 9%; Q3, 14%; Q4, 0%, P<0.001). Multiple LAMRTs (n=10) were induced only in Q1. Among patients with $LVA_{0.1}$ (n=11), ATs were induced in 10 (91%). The inducibility of LAMRT increased as LVA appeared at lower voltage cutoffs (Figure S10). All the critical isthmuses were located in the LVAs except for 4 roof reentrant ATs, which were induced in patients without $LVA_{1.0}$.

Histological Assessment of Atrial Biopsy Samples and Its Relationship With Bipolar Voltage

Atrial biopsy samples were histologically analyzed in 28 patients (indicated by red dots in Figure 1). Patient characteristics of the biopsy group in comparison with the non-biopsy group are shown in Table S6. Examples of a voltage map at the biopsy site, imaging of the biopsy site at the limbus of fossa ovalis (FO) using ICE, and imaging of the bioptome using ICE and fluoroscopy are shown in Figure 5 and Figure S11. The number and the size of samples on the glass slide were 2.4±0.9 and 1.8×1.2 mm per patient. The area of myocardial tissue was 0.76±0.52 mm^2 (range 0.2–1.9 mm^2) after excluding endocardial connective tissue and adipose tissue. Figure 6A shows the algorithm to measure %fibrosis using the image analysis platform. The %fibrosis ranged from 1.2% to 17.0% (7.9±4.4%) with various amounts of interstitial fibrosis (Figure 6B
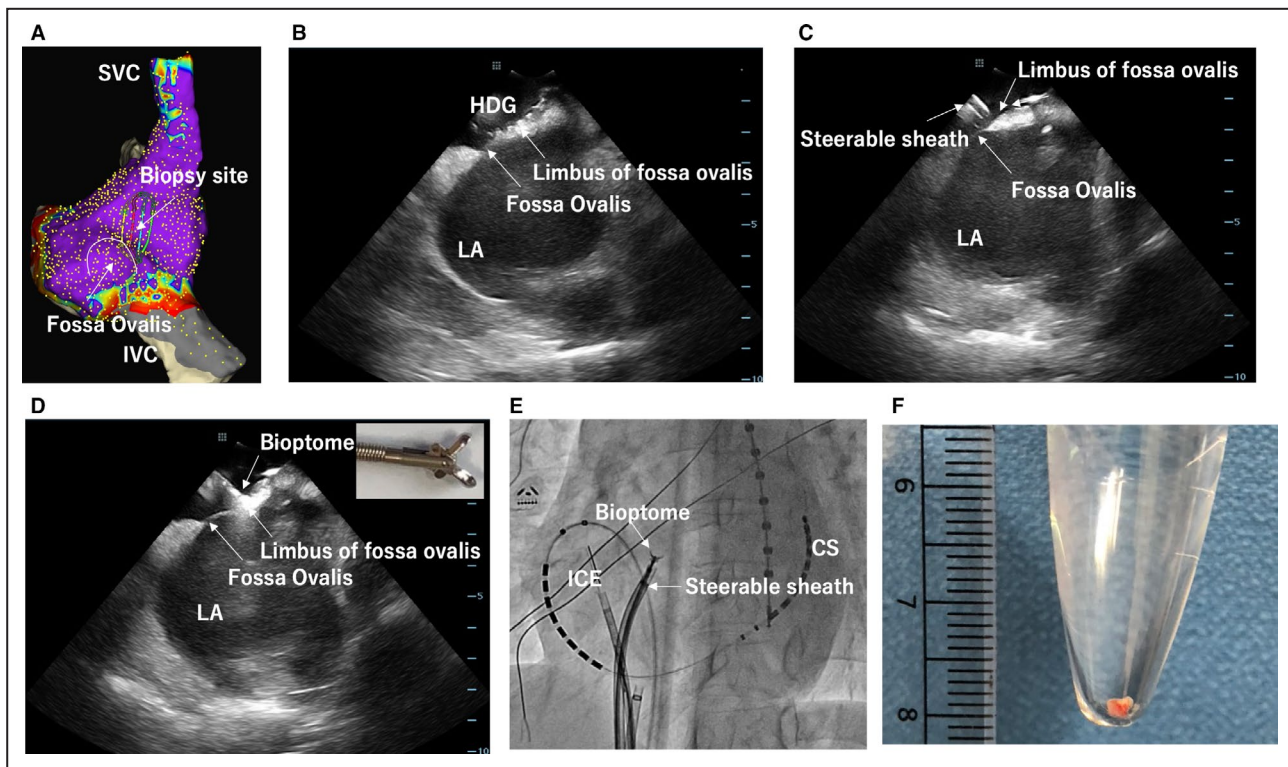
Figure 5. Right atrial septum biopsy.
A, An example of voltage map of the RA septum with a shadow of GMC showing the biopsy site. **B**, An image of intracardiac echocardiography (ICE) showing that GMC was placed at the limbus of the fossa ovalis. **C**, An image of ICE showing a steerable sheath placed near the biopsy site on the limbus of the fossa ovalis. **D**, An image of ICE showing a bioptome directly advanced to the biopsy site through the steerable sheath. **E**, Fluoroscopy viewed from left anterior oblique showing the location of the ICE, steerable sheath, and bioptome. **F**, An example of biopsy sample with 2 mm size. CS indicates coronary sinus; IVC, inferior vena cava; LA, left atrium; RA, right atrium; and SVC, superior vena cava.

through 6J). ICC were calculated for the intra- and inter-observer variability. The ICC were 0.948 and 0.865, respectively.

Examples of voltage map in a patient with minimal fibrosis and a patient with severe fibrosis were shown in Figure 6K (no $LVA_{1.5}$) and 6L (extensive $LVA_{1.5}$). V_{biopsy} decreased and %fibrosis increased as the quartile moved down to the lower quartile (Figure 7). The %fibrosis was inversely correlated both with V_{biopsy} and V_{GLA} ($r=-0.71$ and -0.72, respectively), and V_{biopsy} was positively correlated with V_{GLA} ($r=0.82$) (Figure 7). The V_{biopsy} values of the patients with the minimal (1.2%) and the maximum %fibrosis (17.0%) were 15.0 and 5.6 mV, respectively. The limbus of FO, the biopsy site, had the highest voltage in the RA septum in all 28 patients in the biopsy group (Figure S11). No slow conduction was identified at the biopsy site in any patient. There was a positive linear relationship between V_{FO} and V_{biopsy}: $V_{FO}=-0.8+0.6 \times V_{biopsy}$ ($r=0.700$, $P<0.001$, Figure S12). No complications associated with the biopsy and ablation procedures were noted.

DISCUSSION

Major Findings

The major findings of the present study were as follows: (1) bipolar voltage reduction in the LA of patients with AF is a diffuse process ranging in severity from minimal to severe; (2) the presence and extent of LVAs are closely related to the global LA voltage reduction, no matter which voltage cutoff between 0.1 and 1.5 mV is used; (3) a close relationship between atrial voltage reduction and the extent of fibrosis was confirmed by histology based on atrial biopsy. To the best of our knowledge, this is the first paper to report these findings. These electrophysiological and histological findings also suggest that the presence of LVA is a surrogate for diffuse fibrotic remodeling of the LA, rather than local fibrosis, depending on the voltage cutoff and its extent.

Evidence for a Diffuse Voltage Reduction in the LA

Global LA voltage (V_{GLA}) distributed along a continuum rather than a discontinuous curve, and the V_{RLA} decreased in all anatomical regions of the LA as the V_{GLA}
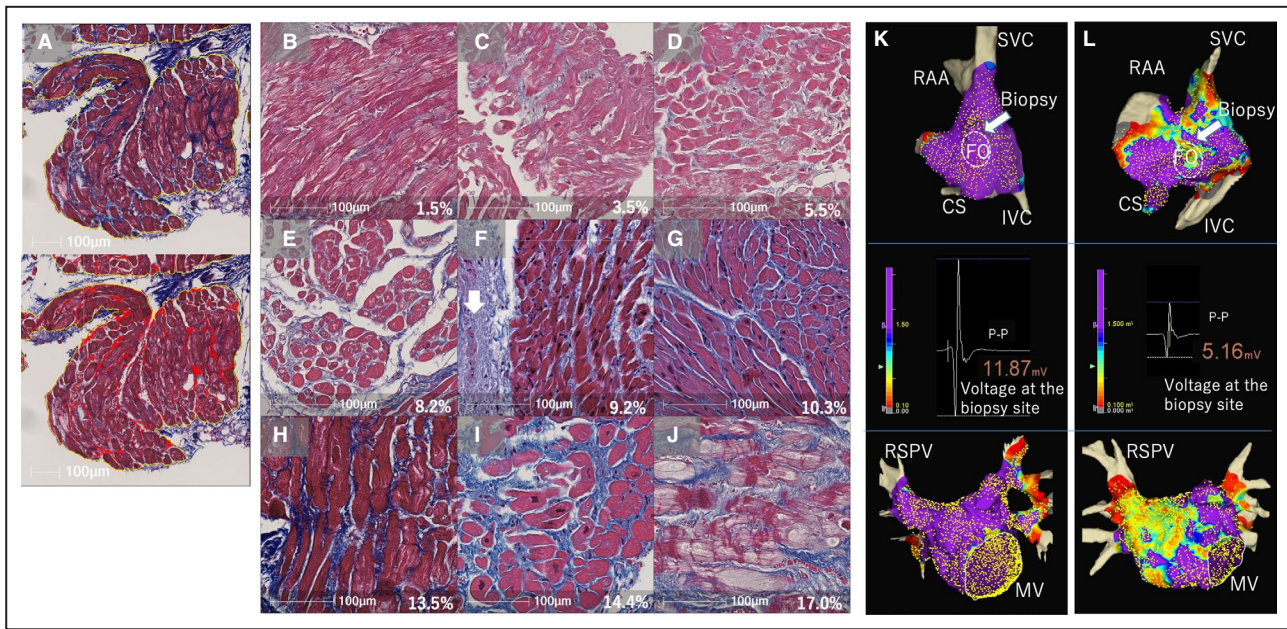
Figure 6. Histological assessment of atrial biopsy samples.
A, A Masson's trichrome stained sample from the right atrial (RA) septum (top) and the algorithm for quantitative analysis of %fibrosis using the image analysis platform (HALO) (bottom). The blue staining in the top indicates fibrosis. Only the area surrounded by the yellow lines, which excludes the endocardial connective tissue and adipose tissue, was analyzed to measure %fibrosis. The blue stained areas were highlighted in red and %fibrosis was calculated by dividing the total red area by the total area surrounded by the yellow line. **B** through **J** are examples of histological images ordered from low to high %fibrosis. Endocardium (white arrow in **F**) and large adipose tissue were excluded from the measurement of %fibrosis. The value in each figure shows %fibrosis. **K**, The voltage map of the RA septum (top) and LA (bottom) of the same patient as in (**B**). There is no LVA (defined as <1.5 mV) and the bipolar voltage at the biopsy site is high (middle). **L**, The voltage map of the RA septum and LA of the same patient as in (**I**). LVAs were identified and the bipolar voltage at the biopsy site was relatively low. The color gradation indicates the serial changes in the voltage amplitude from purple at 1.5 mV to grey at 0.1 mV. CS indicates coronary sinus; f, %fibrosis; FO, fossa ovalis; IVC, inferior vena cava; LVA, low-voltage area; MV, mitral valve; RAA, right atrial appendage; RSPV, right superior pulmonary vein; and SVC, superior vena cava.

decreased. These findings indicate that voltage reduction in the LA is a diffuse phenomenon. Furthermore, there was no significant difference in the relative V_{RLA} with reference to Q4 in all anatomical regions except the lateral wall, suggesting a uniform voltage reduction across the whole LA. The reason why the relative V_{RLA} of the lateral wall is higher than that of other regions is not clear. However, it is possible that the analysis region included a part of the LAA, which has higher voltages.[16] The possibility of non-uniform voltage reduction within individual anatomical regions still remained. Therefore, we evaluated the distribution of voltage values across the whole LA using a histogram, and found that as the quartiles moved down, the histogram shifted toward lower voltages, maintaining a unimodal distribution, indicating that uniform voltage reduction even in individual regions is likely. Schreiber et al[16] reported that the maximum voltage in the LA (in the majority inside the LAA) decreased in those with extensive LVAs compared with those with no or minimum LVAs, suggesting a diffuse atrial remodeling process. However, the study did not show that voltage reduction is a diffuse phenomenon throughout the LA and regarded LVAs as severe local fibrotic areas.

Comparison of Bipolar Voltage Between Q4 and the Control Group

Both V_{GLA} and V_{RLA} in Q4 were comparable to those of the control group without any history of AF or other cardiovascular disease. Both the density curve and cumulative probability curve of the 2 were very similar, suggesting that Q4 is very close to the control group in terms of bipolar voltage. The histological fibrosis of Q4 was 5.1±2.9%. It is not clear whether this degree of fibrosis does not affect the bipolar voltage or whether this degree of fibrosis is also present in the control group, since we did not perform biopsies in the control group. Nevertheless, it can be stated that the severity of voltage reduction in Q4 is minimal, while that in Q1 is severe.

LVA as a Reflection of Diffuse Fibrotic Remodeling in the LA

LVA appeared predominantly in the anterior wall and septum. The distribution of the LVA in this study was consistent with previous studies.[12–17] The primary cause of voltage reduction has been considered as fibrosis,[11–18] although it has never been validated
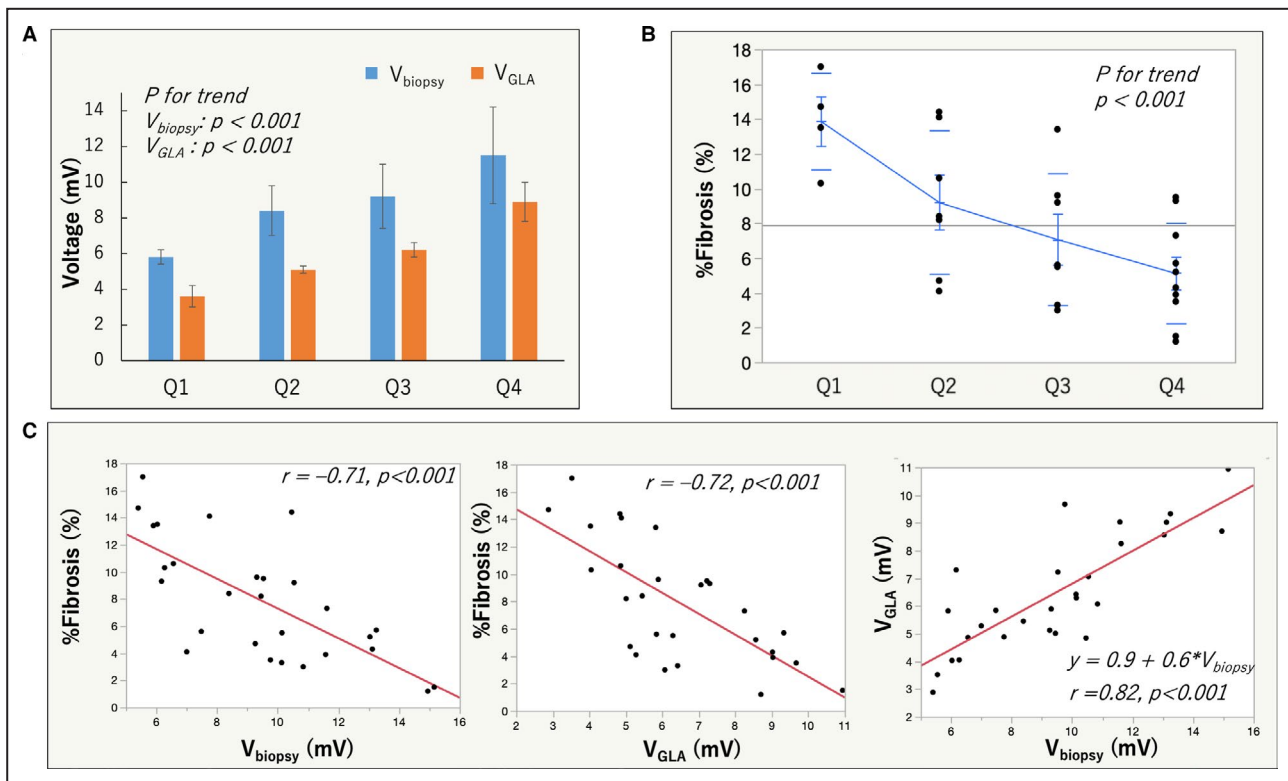
Figure 7. Relationship between atrial voltage reduction and the extent of fibrosis.
A, Mean bipolar voltage at the biopsy site (V_{biopsy}) as well as global LA voltage (V_{GLA}) in each quartile, both of which decreased as the quartiles moved down. **B**, %fibrosis of each quartile in the biopsy group was shown, which also decreased as the quartile moved down. **C**, There were an inverse relationship between V_{biopsy} and %fibrosis (left), between V_{GLA} and %fibrosis (middle), and a positive relationship between V_{biopsy} and V_{GLA}.

histologically. Based on the assumption that local LVA is a local fibrotic area, numerous investigators have considered LVA as a substrate for AF and have also targeted LVA for AF substrate modification.[12–17] However, the present study clearly showed that the presence and extent of LVA reflected a decrease in V_{GLA}. In addition, there were good correlations between V_{biopsy}, V_{GLA}, and the extent of histological fibrosis. This indicates that histological fibrosis is one of the causes of the voltage reduction. However, the previous assumption that a local LVA represents a local fibrotic area seems unlikely, although LVAs may represent regions of greater local fibrosis in the context of diffuse fibrosis, particularly as seen in this study as substrate potentiating LAMRT. Histological evaluation in this study was limited to a small part of the RA septum, and together with the voltage findings of the atria, fibrosis of the whole LA was speculated. On the other hand, Oakes et al[18] showed that there was a correlation between the degree of LGE-MRI and bipolar voltage, and McGann et al[22] reported an association between the region of LGE-MRI and histological fibrosis in surgical biopsy specimens in the LA of 10 patients. Zghaib et al[23] also reported a reasonable agreement between LGE-MRI

and bipolar voltage. Therefore, it cannot be ruled out that fibrosis is a heterogeneous process and that the decrease in voltage is due to local fibrosis. The multimodality correlation of fibrosis across voltage, imaging and histology will be necessary in the future.

The present study indicates that the presence of LVA rather is a surrogate for diffuse fibrotic remodeling of the LA. Based on the assumption that LVA is a local fibrotic lesion, there have been discussions of the optimal cutoff value of LVA for assessment of the presence of fibrotic lesions.[11,24,25] However, based on the findings of the present study that voltage reduction is a diffuse phenomenon, and LVA extent linearly increased as voltage cutoff increased, it is not reasonable to assume a certain cutoff value for the assessment of fibrotic area. Notably, the biopsy sites with the most severe %fibrosis showed a voltage amplitude of 5.6 mV. The linear relationship between V_{biopsy} and V_{GLA} was expressed as $V_{biopsy} = 2.2 + 1.1 \times V_{GLA}$. The limbus of FO, the biopsy site, had the highest voltage in the RA septum in all 28 patients in the biopsy group. In addition, there was a positive linear relationship between V_{FO} and V_{biopsy}: $V_{FO} = -0.8 + 0.6 \times V_{biopsy}$, indicating that V_{FO} was consistently lower than V_{biopsy} at the limbus

Table 1. Patient Characteristics Across Quartiles of Mean LA Voltage

Variables	Q1 (<4.2 mV) n=35	Q2 (4.2–5.6 mV) n=35	Q3 (5.7–7.0 mV) n=35	Q4 (≥7.1 mV) n=35	Control n=13	*P* for trend in Q1–Q4	*P* value, Q4 vs control
Age, y	73±8	71±6	68±8	62±13	55±10	<0.001*	0.059
Females, n (%)	18 (51)	11 (31)	9 (26)	4 (11)	5 (38)	0.001*	0.047*
Non-PAF, n (%)	29 (83)	22 (63)	18 (51)	14 (40)	…	<0.001*	…
BMI, kg/m^2	24.1±3.4	25.3±3.3	24.0±4.1	25.3±3.9	23.9±5.1	0.749	0.358
History of cerebral infarction	4 (11)	1 (3)	4 (11)	3 (9)	0 (0)	1.000	0.552
History of congestive heart failure, n (%)	9 (26)	5 (14)	5 (14)	2 (6)	0 (0)	0.026*	1.000
Hypertension, n (%)	20 (57)	20 (57)	14 (40)	16 (46)	1 (8)	0.173	0.018*
Diabetes, n (%)	6 (17)	4 (11)	4 (11)	9 (26)	1 (8)	0.358	0.247
CHA$_2$DS$_2$-VASc score (IQR)	3 (2–4)	2 (2–3)	2 (1–3)	2 (1–3)	0 (0–1)	<0.001*	0.009*
eGFR, mL/min per 1.73 m^2	51±21	58±18	61±17	65±18	69±9	0.001*	0.242
LVEF, %	61±12	65±11	63±14	70±11	68±7	<0.001*	0.380
LA diameter, mm	42±5	43±6	39±5	38±6	34±6	<0.001*	0.094
LA volume, mL	174±47	169±44	140±38	141±45	…	<0.001*	…
LA volume/BSA, mL/m^2	108±26	99±23	84±19	78±22	…	<0.001*	…
Global LA voltage (V$_{GLA}$), mV	3.0±0.8	4.9±0.4	6.3±0.4	8.5±1.3	8.5±1.0	<0.001*	0.946
Atrial biopsy, n	4	7	7	10	…		…
%fibrosis, %	13.9±2.8	9.2±4.1	7.1±3.8	5.1±2.9	…	<0.001*	…
Voltage at biopsy site, mV	5.8±0.4	8.4±1.4	9.2±1.8	11.8±2.7	…	<0.001*	…

*Significant value (*P* < 0.05).

AT indicates atrial tachycardia; BMI, body mass index; BSA, body surface area; eGFR, estimated glomerular filtration rate; IQR, interquartile range; LA, left atrium; LVEF, left ventricular ejection fraction; PAF, paroxysmal atrial fibrillation; Q1–4, first to fourth quartile; and RA, right atrium.

of FO. These data suggest that the bipolar voltage is inherently different in each region of the RA, and the limbus of FO would be an innately high voltage region. Therefore, it is assumed that a voltage of about 5 mV was recorded at the biopsy site, even in cases of severe fibrosis. It would not be possible to assess the extent of fibrosis with a simple voltage cutoff value. A significant decrease in voltage indicates the presence of fibrosis, but even if the voltage has not decreased to a certain cutoff, it does not mean that fibrosis has not progressed in some regions. These findings are consistent with the previous histological study evaluating post-mortem material reported by Platonov et al,[6] in which the extent of fibrosis did not differ among 5 sampling locations in the atria, including crista terminalis, Bachmann's bundle, inferior PV, posterior LA, and superior PV, showing that fibrosis progression is a diffuse process in the atria. The current study also proved that the V$_{RLA}$ of the anterior and septum is lower than that of other regions even in Q4 and the control group. This indicates that the regional voltage of the anterior wall and septum are innately lower than the other regions. Therefore, LVA appears preferentially in those regions as the global voltage decreases. The reason why the innate voltage varies from region to region could be the fact that the thickness of the atrial wall and the complexity of the myocardial fiber bundles vary from region to region, especially in the anterior and septum.[26,27]

There is a very thin area in the anterior wall just behind the aorta and a very thin-walled foramen ovale in the septum,[26,27] which are thought to be particularly prone to lower voltage.

Factors That Influence Bipolar Voltage

Bipolar voltage depends on the directionality.[20,24] In order to reduce the effect of directional sensitivity, all bipolar signals both along and across the splines of the GMC were collected, and the highest amplitude bipolar signal was displayed on the voltage map. Nevertheless, the effect of directional sensitivity still appears. For example, if the excitation wave propagates from a 45° angle toward the 2 orthogonal electrode pairs, the bipolar voltage recorded at either electrode pair will decrease to the same extent. We evaluated V$_{GLA}$ and V$_{RLA}$ by a mean of the highest voltage at a sampling density of 1 cm^2, which would minimize the impact of directional sensitivity on the measurement of V$_{GLA}$ and V$_{RLA}$. Activation direction and rate of wavefront propagation have been known to influence bipolar voltage, the distribution and extent of LVAs.[28] We compared V$_{GLA}$ during both HRAp and CSp at the same rate of 100 bpm to investigate the impact of different activation directions. There was a small difference in the distribution of LVAs, which is consistent with the previous study.[28] However, the V$_{GLA}$ was almost identical between the 2,

suggesting that V_{GLA} may depend more on the amount of atrial tissue mass than on the activation direction. We did not investigate the impact of pacing cycle length on V_{GLA} and V_{RLA} in this study. It is unknown whether the voltage reduction is consistently diffuse even during pacing at a shorter cycle length. Other factors, such as filtering,[29] catheter incident angle, catheter contact, and tissue thickness, also affect the bipolar voltage. Electrode size and inter-electrode spacing also affect the bipolar voltage.[30] In this study, we compared V_{GLA} between GMC and CMC in a subset of the AF group. There was a strong linear relationship between the 2 mapping catheters, and V_{GLA} by CMC was $0.75 \times V_{GLA}$ by GMC. This finding suggests that voltage strongly depends on the mapping electrodes and that a single binary threshold cannot accurately characterize atrial fibrosis.

Impact of Diffuse Voltage Reduction on the Inducibility of LAMRT

The inducibility of LAMRT increased as the quartile moved down and as the lowest voltage cutoff value at which LVA appeared became lower. In addition, the majority of critical isthmus for the LAMRTs was located in the LVA, suggesting that LVA works as a substrate for LAMRT. Especially, the presence of $LVA_{0.1}$ was closely associated with LAMRT, suggesting that as the voltage decreases, conduction slowing or block appears, creating a substrate for LAMRT. We speculate that the previously reported ablation strategy targeting LVA as a localized fibrotic area may have prophylactically ablated the substrate of AT, which resulted in better arrhythmia free-survival.[12–14,16,17] However, other studies did not show any significant improvement in arrhythmia free-survival.[15,31,32] Since an LVA is not a localized fibrotic area, it is reasonable to assume that the AF substrate cannot be modified by LVA ablation.

Clinical Factors Associated With Lower V_{GLA}

There were significant associations between reduction of V_{GLA} and age, female sex, non-PAF type, history of congestive heart failure, eGFR, LVEF, and LA size in univariate analyses. All these clinical factors have been widely recognized and discussed as predictors of LVA.[10–16] The consistency is as expected because LVA is a reflection of reduction in V_{GLA}. Even though most of the LVAs, generally defined <0.5 mV, were not found in the Q2 and Q3 groups, the correlation between these predictors and the quartile decline suggests that they are related to the process of diffuse voltage reduction. However, due to the small number of patients who underwent histological evaluation in this study, we did not evaluate the association between those clinical factors and histological findings. Future studies are needed to clarify the relationship. There were significant differences in demographic and clinical characteristics between the quartiles and the Q1–Q3 versus control group, which may have influenced the association between V_{GLA} and the presence of LVA. Multiple logistic regression analysis adjusted for covariates significantly associated with V_{GLA} revealed that V_{GLA} independently predicted the presence of LVA at cutoff values of 0.5, 1.0, and 1.5 mV, which suggests that V_{GLA} is significantly associated with the presence of LVA, regardless of the patient's characteristics.

Feasibility of Endomyocardial Atrial Biopsy and Histological Fibrosis in Patients With AF

Histological evaluation of atrial muscle in humans has been mainly based on biopsy specimens from open heart surgery and autopsy cases.[4–6] However, the patients' backgrounds in these studies are different from those of patients undergoing catheter ablation for nonvalvular AF. Endomyocardial biopsies from atria with thin walls are considered to have a higher risk of complications than biopsies from ventricles and have not been commonly performed. Endocardial biopsy from the RA of a beating heart in patients with AF was first reported by Frustaci et al,[3] in which abnormal atrial histology was consistently found in all 12 patients with paroxysmal lone AF. Sepehri Shamloo et al[33] recently reported the feasibility of RA septum biopsy in 4 patients undergoing AF ablation. Both studies included a small number of patients, and neither evaluated fibrosis in relation to bipolar voltage. In this study, a total of 69 patients underwent atrial biopsy without any complications, of which 28 met the inclusion and exclusion criteria and were analyzed. The ICE-guided endocardial biopsy from the RA septum seems to be a feasible and safe technique, although the significance of the RA biopsy in clinical practice is still unclear. We showed an inverse relationship between bipolar voltage and %fibrosis. However, there was variation in %fibrosis, especially in patients whose voltage was in the middle range. Factors other than fibrosis may affect voltage, eg, myocyte cell size, myocyte disarray, intercellular-spacing, myofibrillar loss, infiltration with adipocytes. Due to the limited number of patients with histological evaluations in this study, the impacts of these factors on voltage have not been analyzed, and future studies are warranted.

Limitations

This study has several limitations. First, the voltage mapping was based on the endocardial surface of the LA and the RA septum, and it was not performed in the whole RA, the LAA, and on the epicardial surface. It

is unclear whether the diffuse voltage reduction is also observed in these structures. Second, biopsy was performed only from the RA septum. Therefore, fibrotic remodeling of the LA is only an estimate based on the close relationship between the voltage data and the extent of fibrosis at the biopsy site. Third, the non-biopsy AF group and the control group did not undergo histological evaluation. Therefore, the possibility of amyloid deposition cannot be ruled out in these groups. Fourth, although Masson's trichrome staining was performed by a single technician, differences in the concentration of the staining may have affected the quantification of fibrosis. Fifth, the endocardial connective tissue stained with blue was excluded from the analysis of %fibrosis. However, there were cases in which it was difficult to clearly distinguish the connective tissue from interstitial and perivascular fibrosis, which may have affected the quantification of %fibrosis. Sixth, we did not perform an imaging evaluation of fibrosis using LGE-MRI. LGE-MRI of the atria is available only in a very limited number of research centers and could not be performed in our institution, although the multimodality correlation of fibrosis across voltage, imaging and histology would be of significant interest. Seventh, only 4 patients were classified as Q1 in the biopsy group, and histological evaluation of the patients in Q1 was insufficient; thus, further studies are needed. Eighth, Platonov et al did not analyze fibrosis at the interatrial septum. Therefore, it was just speculation that histological fibrosis would be diffuse and the extent would be similar between the atrial septum and the other locations analyzed by Platonov et al. Ninth, the biopsy cohort consisted of 28 patients, who were selected from 69 consecutive patients undergoing atrial septum biopsy. Most of the exclusion criteria were established to exclude the impact of ablation on the atrial muscle. Among them, 16 patients were excluded because sufficient myocardial tissue could not be obtained. This may be due to the very thick atrial endocardium. The exclusion of a large number of patients in the biopsy group may have affected the results.

CONCLUSIONS

Voltage reduction in the LA of patients with AF is a diffuse process with minimal to maximal severity and is associated with the extent of histological fibrosis. The presence of LVA reflects a diffuse voltage reduction of the LA.

ARTICLE INFORMATION

Affiliations

Department of Cardiovascular Medicine (T.Y., T.O., Y.T., K.Nakashima, K.S., R.O., M.T., K.Node), Department of Advanced Management of Cardiac Arrhythmia (T.Y., T.O.) Education and Research Center for Community Medicine (A.K.) and Department of Pathology and Microbiology (S.A.), Saga University, Saga, Japan; Department of Cardiology and Clinical Examination, Faculty of Medicine, Oita University, Yufu, Japan (A.F., K.H., Y.I., N.T.); and Division of Cardiology, Saiseikai Futsukaichi Hospital, Fukuoka, Japan (Y.K.).

Supplemental Material

Data S1–S2
Tables S1–S6
Figures S1–S12

REFERENCES

1. Dzeshka MS, Lip GY, Snezhitskiy V, Shantsila E. Cardiac fibrosis in patients with atrial fibrillation: mechanisms and clinical implications. *J Am Coll Cardiol*. 2015;66:943–959. doi: 10.1016/j.jacc.2015.06.1313

2. Nattel S, Harada M. Atrial remodeling and atrial fibrillation: recent advances and translational perspectives. *J Am Coll Cardiol*. 2014;63:2335–2345. doi: 10.1016/j.jacc.2014.02.555

3. Frustaci A, Chimenti C, Bellocci F, Morgante E, Russo MA, Maseri A. Histological substrate of atrial biopsies in patients with lone atrial fibrillation. *Circulation*. 1997;96:1180–1184. doi: 10.1161/01.CIR.96.4.1180

4. Goette A, Juenemann G, Peters B, Klein HU, Roessner A, Huth C, Röcken C. Determinants and consequences of atrial fibrosis in patients undergoing open heart surgery. *Cardiovasc Res*. 2002;54:390–396. doi: 10.1016/S0008-6363(02)00251-1

5. Boldt A, Wetzel U, Lauschke J, Weigl J, Gummert J, Hindricks G, Kottkamp H, Dhein S. Fibrosis in left atrial tissue of patients with atrial fibrillation with and without underlying mitral valve disease. *Heart*. 2004;90:400–405. doi: 10.1136/hrt.2003.015347

6. Platonov PG, Mitrofanova LB, Orshanskaya V, Ho SY. Structural abnormalities in atrial walls are associated with presence and persistency of atrial fibrillation but not with age. *J Am Coll Cardiol*. 2011;58:2225–2232. doi: 10.1016/j.jacc.2011.05.061

7. Sanders P, Morton JB, Davidson NC, Spence SJ, Vohra JK, Sparks PB, Kalman JM. Electrical remodeling of the atria in congestive heart failure: electrophysiological and electroanatomic mapping in humans. *Circulation*. 2003;108:1461–1468. doi: 10.1161/01.CIR.0000090688.49283.67

8. Miyamoto K, Tsuchiya T, Narita S, Yamaguchi T, Nagamoto Y, Ando S, Hayashida K, Tanioka Y, Takahashi N. Bipolar electrogram amplitudes in the left atrium are related to local conduction velocity in patients with atrial fibrillation. *Europace*. 2009;11:1597–1605. doi: 10.1093/europace/eup352

9. Verma A, Wazni OM, Marrouche NF, Martin DO, Kilicaslan F, Minor S, Schweikert RA, Saliba W, Cummings J, Burkhardt JD, et al. Pre-existent left atrial scarring in patients undergoing pulmonary vein antrum isolation: an independent predictor of procedural failure. *J Am Coll Cardiol*. 2005;45:285–292. doi: 10.1016/j.jacc.2004.10.035

10. Yamaguchi T, Tsuchiya T, Nagamoto Y, Miyamoto K, Murotani K, Okishige K, Takahashi N. Long-term results of pulmonary vein antrum isolation in patients with atrial fibrillation: an analysis in regards to substrates and pulmonary vein reconnections. *Europace*. 2014;16:511–520. doi: 10.1093/europace/eut265

11. Vlachos K, Efremidis M, Letsas KP, Bazoukis G, Martin R, Kalafateli M, Lioni L, Georgopoulos S, Saplaouras A, Efremidis T, et al. Low-voltage

areas detected by high-density electroanatomical mapping predict recurrence after ablation for paroxysmal atrial fibrillation. *J Cardiovasc Electrophysiol.* 2017;28:1393–1402. doi: 10.1111/jce.13321

12. Rolf S, Kircher S, Arya A, Eitel C, Sommer P, Richter S, Gaspar T, Bollmann A, Altmann D, Piedra C, et al. Tailored atrial substrate modification based on low-voltage areas in catheter ablation of atrial fibrillation. *Circ Arrhythm Electrophysiol.* 2014;7:825–833. doi: 10.1161/CIRCEP.113.001251

13. Kottkamp H, Berg J, Bender R, Rieger A, Schreiber D. Box isolation of fibrotic areas (BIFA): a patient-tailored substrate modification approach for ablation of atrial fibrillation. *J Cardiovasc Electrophysiol.* 2016;27:22–30. doi: 10.1111/jce.12870

14. Yamaguchi T, Tsuchiya T, Nakahara S, Fukui A, Nagamoto Y, Murotani K, Eshima K, Takahashi N. Efficacy of left atrial voltage-based catheter ablation of persistent atrial fibrillation. *J Cardiovasc Electrophysiol.* 2016;27:1055–1063. doi: 10.1111/jce.13019

15. Yang G, Yang B, Wei Y, Zhang F, Ju W, Chen H, Li M, Gu K, Lin Y, Wang B, et al. Catheter ablation of nonparoxysmal atrial fibrillation using electrophysiologically guided substrate modification during sinus rhythm after pulmonary vein isolation. *Circ Arrhythm Electrophysiol.* 2016;9:e003382. doi: 10.1161/CIRCEP.115.003382

16. Schreiber D, Rieger A, Moser F, Kottkamp H. Catheter ablation of atrial fibrillation with box isolation of fibrotic areas: lessons on fibrosis distribution and extent, clinical characteristics, and their impact on long-term outcome. *J Cardiovasc Electrophysiol.* 2017;28:971–983. doi: 10.1111/jce.13278

17. Kircher S, Arya A, Altmann D, Rolf S, Bollmann A, Sommer P, Dagres N, Richter S, Breithardt OA, Dinov B, et al. Individually tailored vs. standardized substrate modification during radiofrequency catheter ablation for atrial fibrillation: a randomized study. *Europace.* 2018;20:1766–1775. doi: 10.1093/europace/eux310

18. Oakes RS, Badger TJ, Kholmovski EG, Akoum N, Burgon NS, Fish EN, Blauer JJE, Rao SN, DiBella EVR, Segerson NM, et al. Detection and quantification of left atrial structural remodeling with delayed-enhancement magnetic resonance imaging in patients with atrial fibrillation. *Circulation.* 2009;119:1758–1767. doi: 10.1161/CIRCULATIONAHA.108.811877

19. Masuda M, Asai M, Iida O, Okamoto S, Ishihara T, Nanto K, Kanda T, Tsujimura T, Matsuda Y, Okuno S, et al. Left atrial voltage mapping with a direction-independent grid catheter: comparison with a conventional circular mapping catheter. *J Cardiovasc Electrophysiol.* 2019;30:2834–2840. doi: 10.1111/jce.14263

20. Gaeta S, Bahnson TD, Henriquez C. Mechanism and magnitude of bipolar electrogram directional sensitivity: characterizing underlying determinants of bipolar amplitude. *Heart Rhythm.* 2020;17:777–785. doi: 10.1016/j.hrthm.2019.12.010

21. Kishima H, Mine T, Fukuhara E, Takahashi S, Ishihara M. Is the abnormal conduction zone of the left atrium a precursor to a low voltage area in patients with atrial fibrillation? *J Cardiovasc Electrophysiol.* 2020;31:2874–2882. doi: 10.1111/jce.14744

22. McGann C, Akoum N, Patel A, Kholmovski E, Revelo P, Damal K, Wilson B, Cates J, Harrison A, Ranjan R, et al. Atrial fibrillation ablation outcome is predicted by left atrial remodeling on MRI. *Circ Arrhythm Electrophysiol.* 2014;7:23–30. doi: 10.1161/CIRCEP.113.000689

23. Zghaib T, Keramati A, Chrispin J, Huang D, Balouch MA, Ciuffo L, Berger RD, Marine JE, Ashikaga H, Calkins H, et al. Multimodal examination of atrial fibrillation substrate: correlation of left atrial bipolar voltage using multi-electrode fast automated mapping, point-by-point mapping, and magnetic resonance image intensity ratio. *JACC Clin Electrophysiol.* 2018;4:59–68. doi: 10.1016/j.jacep.2017.10.010

24. Yamaguchi T, Fukui A, Node K. Bipolar voltage mapping for the evaluation of atrial substrate: can we overcome the challenge of directionality? *J Atr Fibrillation.* 2019;11:2116. doi: 10.4022/jafib.2116

25. Al-Kaisey AM, Parameswaran R, Kalman JM. Atrial fibrillation structural substrates: aetiology, identification and implications. *Arrhythm Electrophysiol Rev.* 2020;9:113–120. doi: 10.15420/aer.2020.19

26. Ho SY, Cabrera JA, Sanchez-Quintana D. Left atrial anatomy revisited. *Circ Arrhythm Electrophysiol.* 2012;5:220–228. doi: 10.1161/CIRCEP.111.962720

27. Pashakhanloo F, Herzka DA, Ashikaga H, Mori S, Gai N, Bluemke DA, Trayanova NA, McVeigh ER. Myofiber architecture of the human atria as revealed by submillimeter diffusion tensor imaging. *Circ Arrhythm Electrophysiol.* 2016;9:e004133. doi: 10.1161/CIRCEP.116.004133

28. Wong GR, Nalliah CJ, Lee G, Voskoboinik A, Prabhu S, Parameswaran R, Sugumar H, Anderson RD, McLellan A, Ling L-H, et al. Dynamic atrial substrate during high-density mapping of paroxysmal and persistent AF: implications for substrate ablation. *JACC Clin Electrophysiol.* 2019;5:1265–1277. doi: 10.1016/j.jacep.2019.06.002

29. Lin Y-J, Tai C-T, Lo L-W, Udyavar AR, Chang S-L, Wongcharoen W, Tuan T-C, Hu Y-F, Chiang S-J, Chen Y-J, et al. Optimal electrogram voltage recording technique for detecting the acute ablative tissue injury in the human right atrium. *J Cardiovasc Electrophysiol.* 2007;18:617–622. doi: 10.1111/j.1540-8167.2007.00803.x

30. Anter E, Tschabrunn CM, Josephson ME. High-resolution mapping of scar-related atrial arrhythmias using smaller electrodes with closer interelectrode spacing. *Circ Arrhythm Electrophysiol.* 2015;8:537–545. doi: 10.1161/CIRCEP.114.002737

31. Kumagai K, Toyama H, Zhang B. Effects of additional ablation of low-voltage areas after Box isolation for persistent atrial fibrillation. *J Arrhythm.* 2019;35:197–204. doi: 10.1002/joa3.12169

32. Masuda M, Asai M, Iida O, Okamoto S, Ishihara T, Nanto K, Kanda T, Tsujimura T, Matsuda Y, Okuno S, et al. Additional low-voltage-area ablation in patients with paroxysmal atrial fibrillation: results of the randomized controlled VOLCANO Trial. *J Am Heart Assoc.* 2020;9:e015927. doi: 10.1161/JAHA.120.015927

33. Sepehri Shamloo A, Husser D, Buettner P, Klingel K, Hindricks G, Bollmann A. Atrial septum biopsy for direct substrate characterization in atrial fibrillation. *J Cardiovasc Electrophysiol.* 2020;31:308–312. doi: 10.1111/jce.14308

Supplemental Material

Data S1. A method for subdividing the atria into six regions

First, the boundary between the anterior wall and the roof was defined as the line connecting the 10 o'clock direction of the right superior PV antrum and the 2 o'clock direction of the left superior PV antrum, viewed from the endocardial side. The boundary between the anterior wall and the septum was defined as the line connecting the 10 o'clock direction of the right superior PV antrum and the 10 o'clock direction of the mitral annulus. The boundary between the anterior and lateral walls was defined as a line from the left superior PV at 2 o'clock, through the base of the left atrial appendage, to the mitral annulus at 2 o'clock. The boundary between the septum and the inferior wall was defined as a line from 7 o'clock of the right inferior PV to 7 o'clock of the mitral annulus. The boundary between the roof and the posterior wall was defined as a line from 2 o'clock of the right superior PV to 10 o'clock of the left superior PV, viewed from the endocardial side. The boundary between the posterior wall and the inferior wall was defined as the line connecting the 5 o'clock direction of the right inferior PV and the 7 o'clock direction of the left inferior PV. The boundary between the inferior wall and the lateral wall was defined as the line connecting the 6 o'clock direction of the left lower PV and the 4 o'clock direction of the mitral annulus. An example of subdivision of the LA was shown in Figure 1B.

Data S2. Assessment of intra-observer and inter-observer variability of the segregation

For the assessment of intra-observer variability of the segregation, one observer measured twice the areas of each of the six regions in 25 subjects: five randomly selected subjects from each quartile of the AF group and the control group. The results showed that the mean ICC for the intra-observer variability was 0.826 (0.877 for the anterior wall, 0.820 for the septum, 0.791 for the roof, 0.860 for the inferior wall, 0.745 for the posterior wall, and 0.864 for the lateral wall). In addition, for the assessment of inter-observer variability of the segregation, two independent observers measured the areas of the six regions once each in the 25 subjects. The results showed that the mean ICC for the inter-observer variability was 0.667 (0.596 for the anterior wall, 0.872 for the septum, 0.575 for the roof, 0.617 for the inferior wall, 0.771 for the posterior wall, and 0.572 for the lateral wall)

Table S1. Demographic and clinical factors associated with global LA voltage in the AF group (n = 140)

Variables	Univariate			Multivariate 1		Multivariate 2	
	Coefficients	β	P value	β	P value	β	P value
Age	−0.097	−0.439	< 0.001*	−0.374	< 0.001*	−0.404	< 0.001*
Female	−1.756	−0.371	< 0.001*	−0.433	< 0.001*	−0.467	< 0.001*
Non-PAF, n (%)	−1.394	−0.316	< 0.001*	−0.332	< 0.001*	−0.322	< 0.001*
History of cerebral infarction	−0.015	−0.001	0.981	0.061	0.331	−0.001	0.983
History of congestive heart failure, n (%)	−1.335	−0.221	0.008*	−0.067	0.346	−0.059	0.399
Hypertension, n (%)	−0.519	−0.120	0.157	0.039	0.537	0.059	0.335
Diabetes, n (%)	0.231	0.039	0.642	−0.008	0.894	−0.030	0.620
eGFR, ml/min/1.73m^2	0.030	0.268	0.001*	0.073	0.285	0.059	0.364
LVEF, %	0.036	0.209	0.013*	0.114	0.122	0.095	0.189
LA diameter	−0.119	−0.336	< 0.001*	−0.134	0.068	–	–
LA volume, ml	−0.013	−0.260	< 0.001*	–	–	−0.204	0.006*
Adjusted R^2				0.493		0.525	

*Significant value (*P* <0.05)

eGFR = estimated glomerular filtration rate; LA = left atrium; LVEF = left ventricular ejection fraction; PAF = paroxysmal atrial fibrillation

β = β-coefficients

Table S2. Relationships between global and regional LA voltage

y axis / x axis	Global LA Voltage (V_{GLA})	Regional LA Voltage (V_{RLA})					
		Anterior	Septum	Roof	Inferior	Posterior	Lateral
Global LA Voltage (V_{GLA})		r = 0.91 y = −0.5+0.8x	r = 0.89 y = −0.2+0.8x	r = 0.82 y = −0.1+0.9x	r = 0.92 y = 0.2+1.1x	r = 0.90 y = −0.4+1.3x	r = 0.81 y = 1.7+1.1x
Regional LA Voltage (V_{RLA}) — Anterior	r = 0.91 y = 1.5+1.0x		r = 0.81 y = 1.0+0.8x	r = 0.75 y = 1.2+0.9x	r = 0.79 y = 2.2+1.1x	r = 0.75 y = 1.9+1.2x	r = 0.75 y = 3.2+1.0x
Septal	r = 0.89 y = 1.3+1.0x	r = 0.81 y = 0.6+0.8x		r = 0.74 y = 1.0+0.9x	r = 0.77 y = 2.0+1.1x	r = 0.78 y = 1.4+1.2x	r = 0.64 y = 3.6+0.9x
Roof	r = 0.82 y = 1.9+0.7x	r = 0.75 y = 1.1+0.6x	r = 0.74 y = 1.3+0.6x		r = 0.71 y = 2.7+0.8x	r = 0. 77 y = 1.8+1.0x	r = 0.62 y = 4.0+0.7x
Inferior	r = 0.92 y = 0.7+0.7x	r = 0.79 y = 0.3+0.6x	r = 0.77 y = 0.6+0.6x	r = 0.71 y = 0.8+0.6x		r = 0.79 y = 0.8+0.9x	r = 0.75 y = 2.4+0.8x
Posterior	r = 0.90 y=1.3+0.6x	r = 0.75 y = 0.9+0.5x	r = 0.78 y = 1.0+0.5x	r = 0.77 y = 0.9+0.6x	r = 0.79 y = 2.0+0.7x		r = 0.68 y = 3.5+0.6x
Lateral	r = 0.81 y = 0.8+0.6x	r = 0.75 y = 0.2+0.5x	r = 0.64 y = 0.9+0.4x	r = 0.62 y = 1.0+0.5x	r = 0.75 y = 1.2+0.7x	r = 0.68 y = 1.1+0.7x	

All of the p values are < 0.001, LA = left atrium

Data of the shaded row is presented in Figure S3.

Table S3. Relationship between presence of LVA and global LA voltage before and after covariate adjustment in the AF group

	LVA$_{0.1}$ (n = 11)			LVA$_{0.5}$ (n = 18)			LVA$_{1.0}$ (n = 49)			LVA$_{1.5}$ (n = 85)		
	OR	95% CI	p	OR	95% CI	p	OR	95% CI	p	OR	95% CI	p
Covariate adjustment (−)												
Global LA voltage	0.116	0.04–0.308	<0.001*	0.116	0.308–8.553	<0.001*	0.371	0.263–0.523	<0.001*	0.340	0.235–0.493	<0.001*
Covariate adjustment (+)												
Global LA voltage	−	−	−	0.125	0.036–0.425	<0.001*	0.420	0.276–0.640	<0.001*	0.325	0.200–0.526	<0.001*
Age	−	−	−	1.139	0.974–1.331	0.067	1.070	0.994–1.153	0.062	0.980	0.919–1.046	0.551
Female	−	−	−	3.559	0.329–38.473	0.298	0.741	0.198–2.769	0.655	0.766	0.209–2.808	0.687
Non-PAF	−	−	−	1.279	0.052–31.271	0.879	2.465	0.705–8.622	0.152	1.088	0.309–3.826	0.894
LA volume	−	−	−	1.028	1.001–1.055	0.018*	1.003	0.990–1.016	0.583	1.021	1.006–1.036	0.003*

*Significant value (P <0.05)

CI = confidence interval; LA = left atrium; LVA = low-voltage area; OR = odds ratio; PAF = paroxysmal atrial fibrillation

LVA$_{0.1}$ logistic model was unstable due to limited number of patients with LVA$_{0.1}$.

Table S4. Patient characteristics of those who underwent voltage mapping during coronary sinus pacing

Variables	n = 35
Age, years	72 ± 6
Females, n (%)	13 (37)
Non-PAF, n (%)	22 (63)
BMI, kg/m^2	24.5 ± 4.1
History of cerebral infraction	1 (3)
History of congestive heart failure, n (%)	4 (11)
Hypertension, n (%)	19 (54)
Diabetes, n (%)	7 (20)
CHA$_2$DS$_2$-VASc score (IQR)	2 (2–4)
eGFR, ml/min/1.73m^2	53 ± 18
LVEF, %	67 ± 10
LA diameter, mm	41 ± 6
LA volume, ml	152 ± 43
LA volume/BSA, ml/m^2	93 ± 27
Mean LA voltage, mV	5.5 ± 2.1

AT = atrial tachycardia; BMI = body mass index; BSA = body surface area; eGFR = estimated glomerular filtration rate;

IQR = interquartile range; LA = left atrium; LVEF = left ventricular ejection fraction; PAF = paroxysmal atrial fibrillation

Table S5. Comparison between patients receiving amiodarone and those not receiving in Q1

Variables	Amiodarone (+), n = 8	Amiodarone (−), n = 27	p value
Age, years	74 ± 7	69 ± 10	0.251
Female, n (%)	3 (38)	15 (56)	0.443
Non-PAF, n (%)	8 (100)	21 (78)	0.299
History of congestive heart failure, n (%)	3 (38)	6 (22)	0.396
Hypertension, n (%)	2 (25)	18 (67)	0.051
Diabetes, n (%)	0 (0)	6 (22)	0.299
eGFR, ml/min/1.73m^2	39 ± 22	55 ± 20	0.085
LVEF, %	63 ± 10	61 ± 12	0.511
LA volume, ml	192 ± 64	168 ± 40	0.347
Mean LA voltage, mV	3.1 ± 0.8	3.0 ± 0.8	0.669
Regional LA voltage, mV			
Anterior	2.2 ± 0.9	1.8 ± 0.8	0.236
Septum	2.4 ± 0.6	2.3 ± 0.8	0.699
Roof	2.7 ± 0.8	2.3 ± 0.9	0.303
Inferior	3.6 ± 1.0	3.6 ± 1.2	0.947
Posterior	3.5 ± 1.3	3.5 ± 1.4	0.985
Lateral	5.5 ± 2.4	4.7 ± 1.6	0.373
Presence of LVA$_{0.1}$, n (%)	2 (25)	9 (33)	1.000
Presence of LVA$_{0.5}$, n (%)	4 (50)	13 (48)	1.000
Presence of LVA$_{1.0}$, n (%)	6 (75)	22 (81)	0.647
Presence of LVA$_{1.5}$, n (%)	8 (100)	27 (100)	−

eGFR = estimated glomerular filtration rate; LA = left atrium; LVA = low-voltage area; LVEF = left ventricular ejection fraction; PAF = paroxysmal atrial fibrillation

Table S6. Patient characteristics in the Non-biopsy and Biopsy groups

Variables	Non-biopsy n = 112	Biopsy n = 28	*P* value
Age, years	68 ± 10	70 ± 10	0.593
Female, n (%)	37 (33)	5 (18)	0.103
Non-PAF, n (%)	66 (59)	17 (61)	0.863
BMI, kg/m^2	24.4 ± 3.7	25.7 ± 3.5	0.076
History of cerebral infraction	11 (10)	1 (4)	0.459
History of congestive heart failure, n (%)	18 (16)	3 (11)	0.569
Hypertension, n (%)	52 (46)	19 (68)	0.040*
Diabetes, n (%)	18 (16)	5 (18)	0.821
CHA$_2$DS$_2$-VASc score (IQR)	2 (1–3)	2 (1–3)	0.866
eGFR, ml/min/1.73m^2	59 ± 19	57 ± 18	0.657
LVEF, %	65 ± 13	65 ± 12	1.000
LA diameter, mm	41 ± 6	42 ± 7	0.478
LA volume, ml	155 ± 46	163 ± 49	0.415
LA volume/BSA, ml/m^2	93 ± 26	93 ± 25	0.994
Mean LA voltage, mV	5.5 ± 2.1	6.3 ± 2.3	0.069

AT = atrial tachycardia; BMI = body mass index; BSA = body surface area; eGFR = estimated glomerular filtration rate;

IQR = interquartile range; LA = left atrium; LVEF = left ventricular ejection fraction; PAF = paroxysmal atrial fibrillation

Figure S1. The global left atrial voltage (V_{GLA}) evaluated by the 1 cm^2-area method showed a strong positive correlation with those evaluated by the all-annotated-point method.
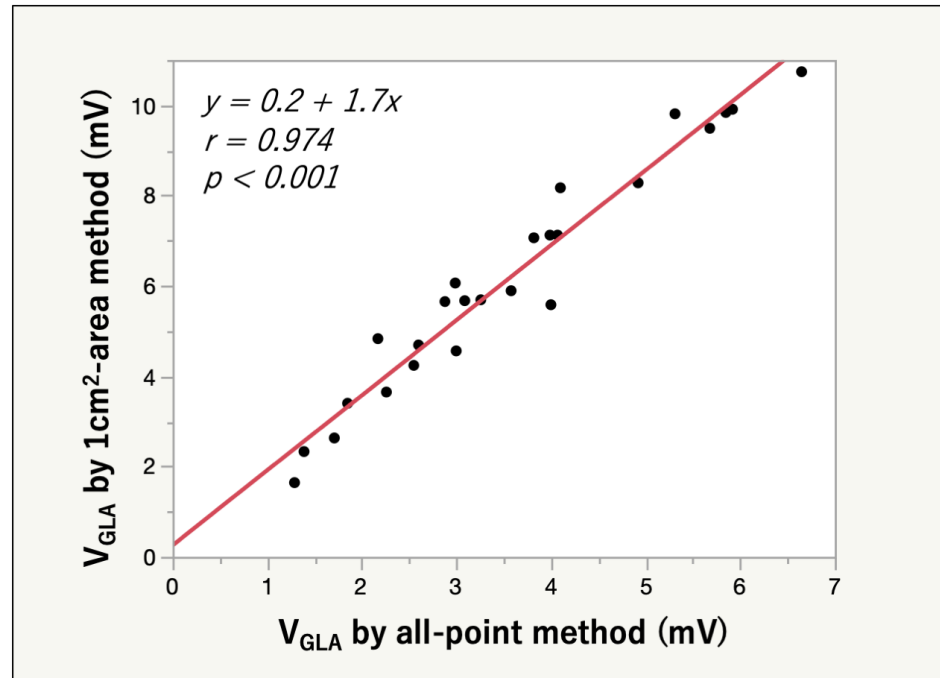
Figure S2. The reginal left atrial voltage (V$_{RLA}$) evaluated by the 1 cm^2-area method showed strong positive correlations with those evaluated by the all-annotated-point method in all regions.
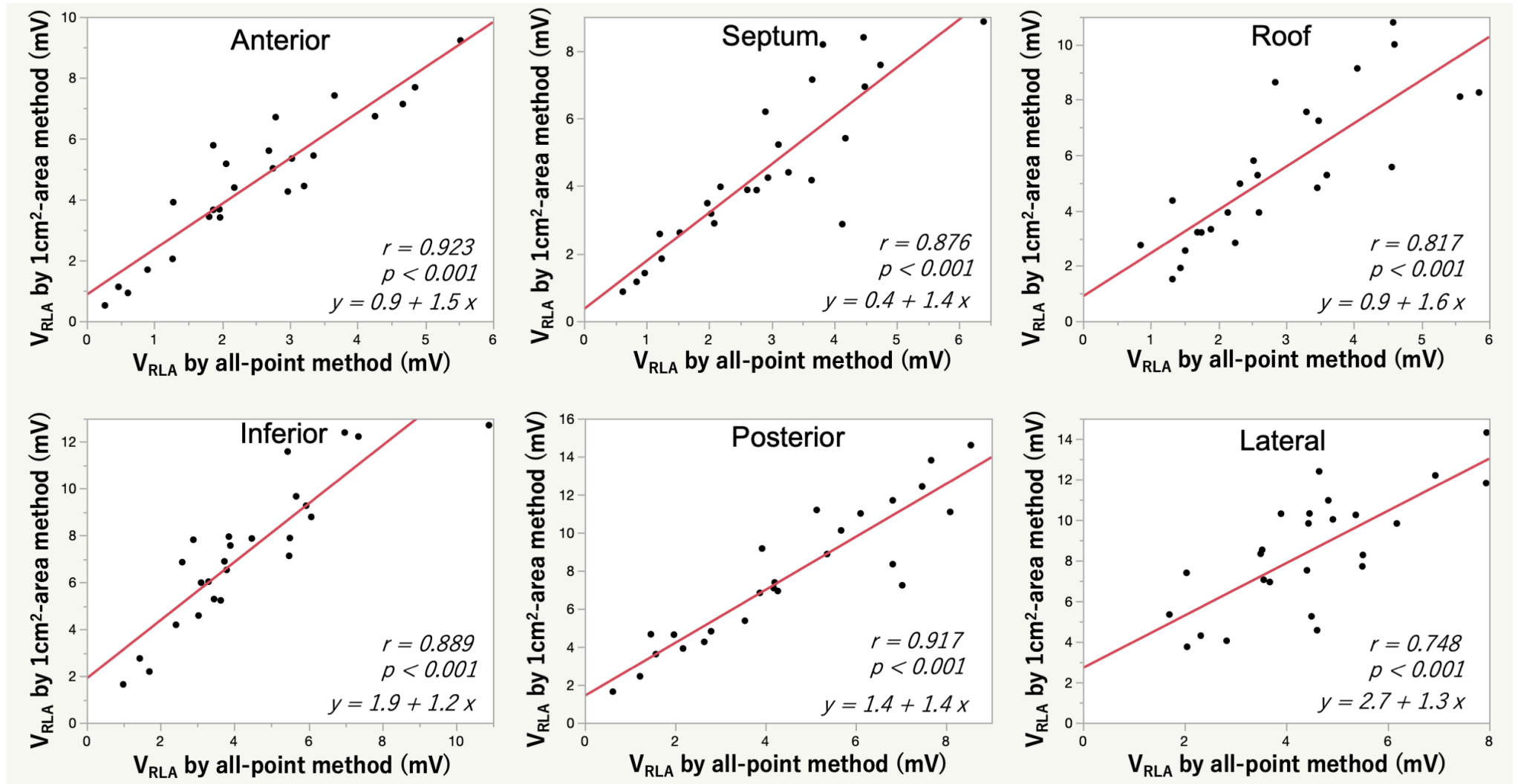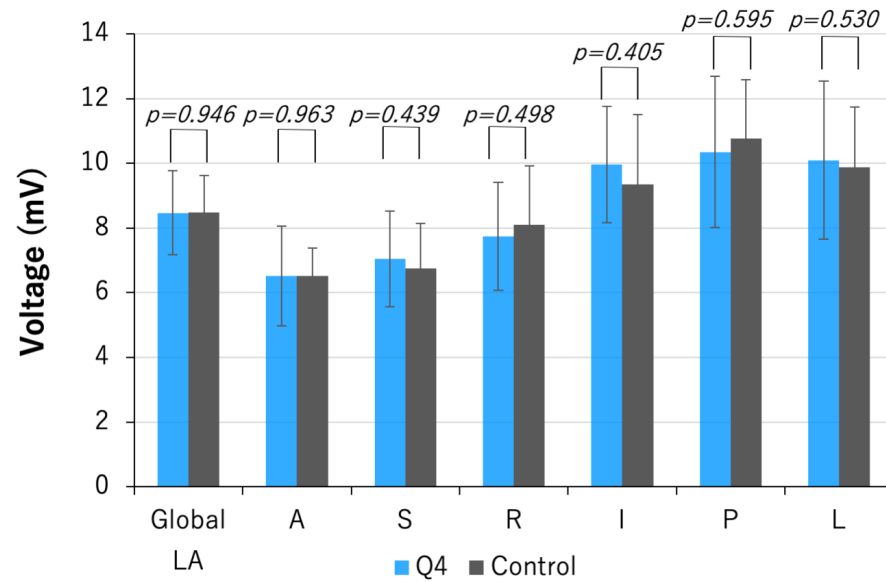
Figure S3. Comparison of V_{GLA} and V_{RLA} between Q4 and the control group. There were no significant differences in V_{GLA} and V_{RLA} at any region between Q4

and the control group. LA, left atrium; V_{GLA}, global LA voltage; V_{RLA}, regional LA voltage

A = Anterior; S = Septum; R = Roof; I = Inferior; P = Posterior; L = Lateral

Figure S4. Comparison of relative regional LA voltage (V_{RLA}) in the AF group. The radar chart consists of the mean of relative V_{RLA} of each anatomical region in Q1 to Q3, which was calculated by the formula in the figure. The relative V_{RLA} at any region decreased as the quartile moved down. The ANOVA showed no significant differences between the anatomical regions at any quartile when the lateral wall was excluded. The value of mean V_{RLA} of each anatomical region in Q4 is also shown in the figure. ANOVA, analysis of variance; LA, left atrium; V_{RLA}, regional LA voltage
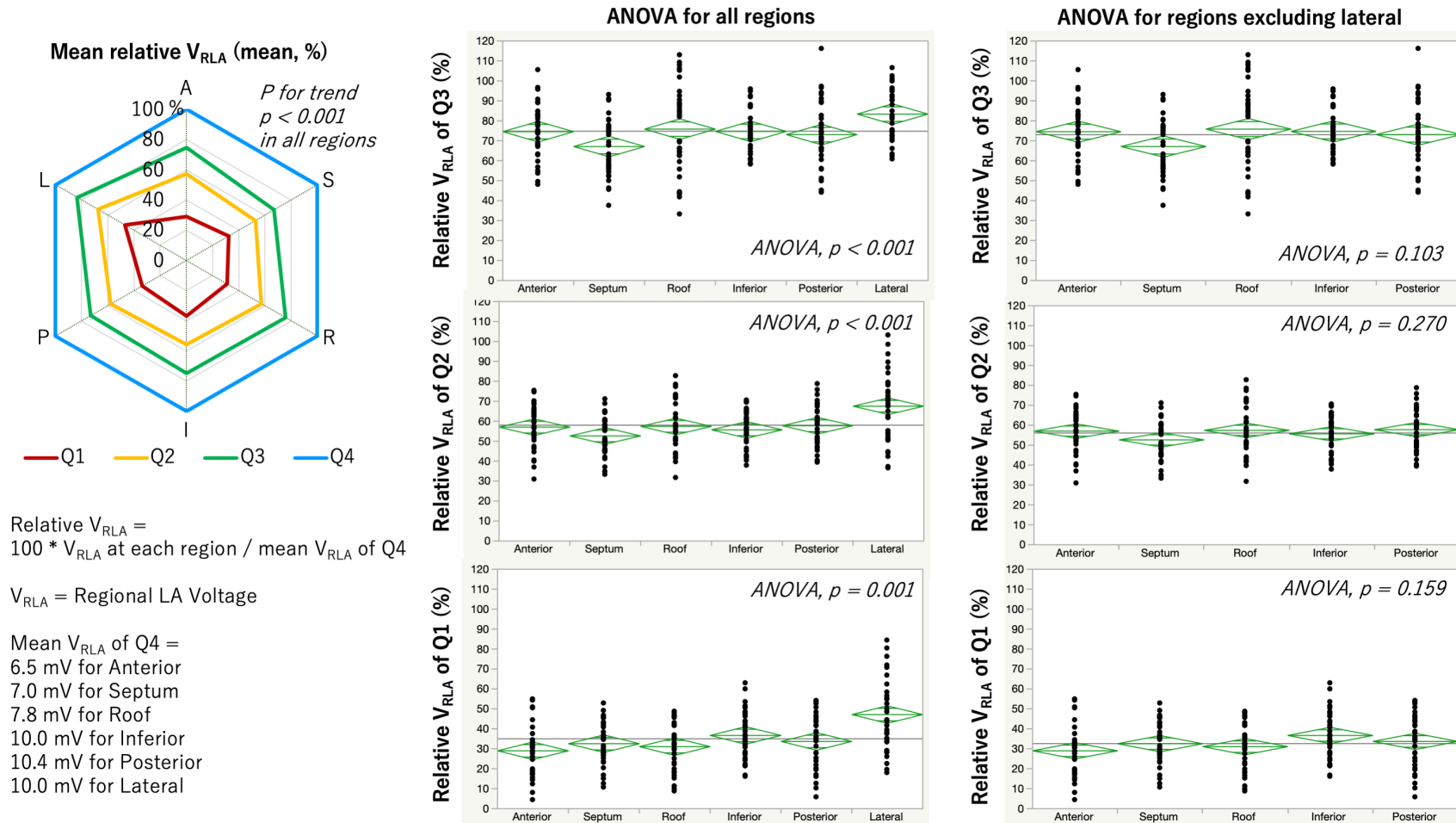
Figure S5. Comparison of regional LA voltage (V_{RLA}) of the anterior wall with the global LA voltage (V_{GLA}) and with the V_{RLA} of other regions. The V_{RLA} of the anterior linearly correlated not only with V_{GLA} but also with the V_{RLA} of other regions. Each dot shows data of each patient. LA, left atrium
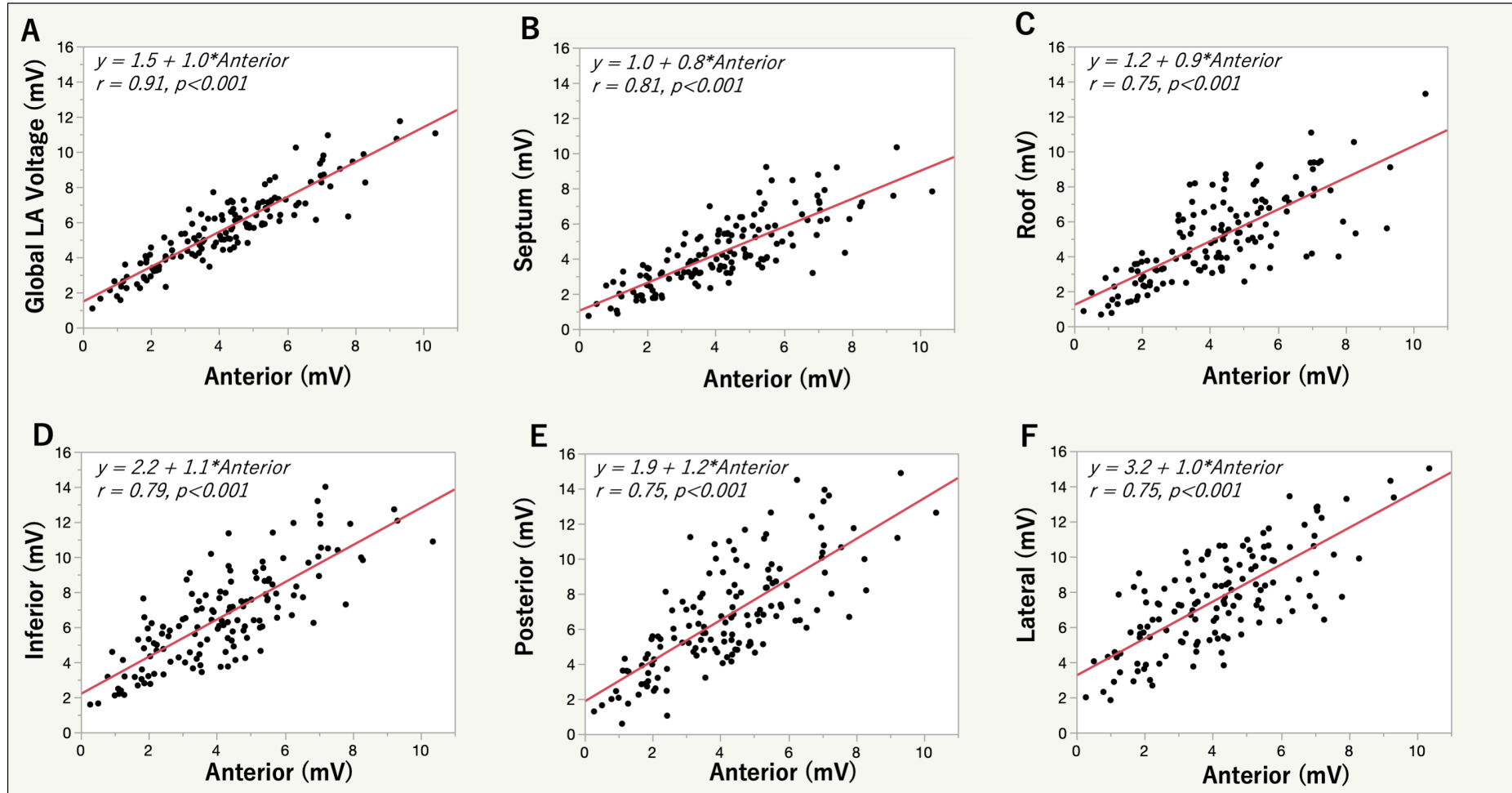

A
$y = 1.5 + 1.0*Anterior$
$r = 0.91, p<0.001$
Global LA Voltage (mV)
Anterior (mV)

B
$y = 1.0 + 0.8*Anterior$
$r = 0.81, p<0.001$
Septum (mV)
Anterior (mV)

C
$y = 1.2 + 0.9*Anterior$
$r = 0.75, p<0.001$
Roof (mV)
Anterior (mV)

D
$y = 2.2 + 1.1*Anterior$
$r = 0.79, p<0.001$
Inferior (mV)
Anterior (mV)

E
$y = 1.9 + 1.2*Anterior$
$r = 0.75, p<0.001$
Posterior (mV)
Anterior (mV)

F
$y = 3.2 + 1.0*Anterior$
$r = 0.75, p<0.001$
Lateral (mV)
Anterior (mV)

Figure S6. Comparison between the global LA voltage (V_{GLA}), evaluated by a mean of the highest voltage at a sampling density of $1\ cm^2$, and the median of

that. Each dot shows data of each patient. There was a strong linear relationship between them. LA, left atrium
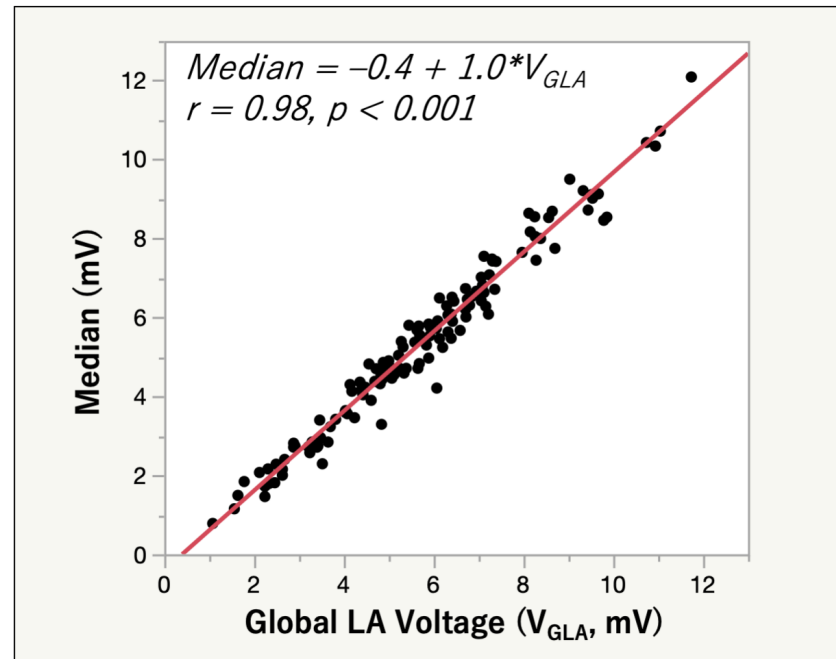
Figure S7. Relationship between the voltage cutoffs of 0.5, 0.75, 1.0, 1.25, and 1.5mV and the LVA extent in the LA at each cutoff in 22 patients with $LVA_{0.5}$ identified. **A**, LVA extent linearly increased as the voltage cutoff increased. **B** and **C**, examples of voltage map at different cutoffs in two patients. LA, left atrium; LAA, left atrial appendage; LSPV, left superior pulmonary vein; LVA, low-voltage area; MV, mitral valve; RSPV, right superior pulmonary vein.
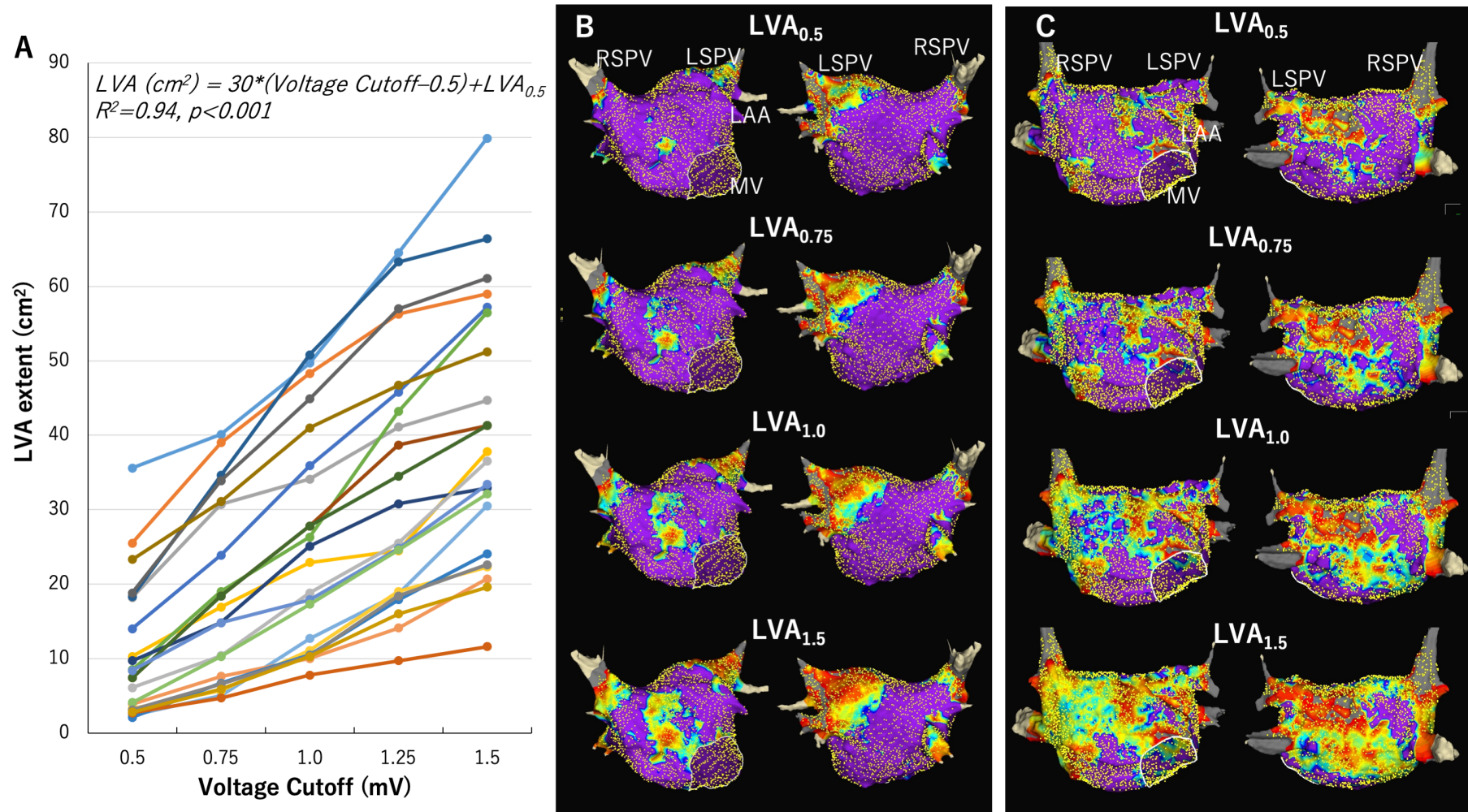
In figure panel A:

$$LVA\ (cm^2) = 30*(Voltage\ Cutoff-0.5)+LVA_{0.5}$$
$$R^2=0.94,\ p<0.001$$

Figure S8. Comparison of an LA voltage map between HRA and CS pacing. A, an example of a same patient during HRA pacing (left) and CS pacing (right) viewed from anterior-posterior and posterior-anterior directions. There was a small difference in the distribution of LVA especially in the posterior wall. **B** to **E**, the relationship of global LA voltage and regional voltages between RAA pacing and CS pacing. There were strong linear relationships. CS, Coronary sinus; HRA, high right atrium; LA, left atrium; LAA, left atrial appendage; LSPV, left superior pulmonary vein; LVA, low-voltage area; MV, mitral valve; RSPV, right superior pulmonary vein.
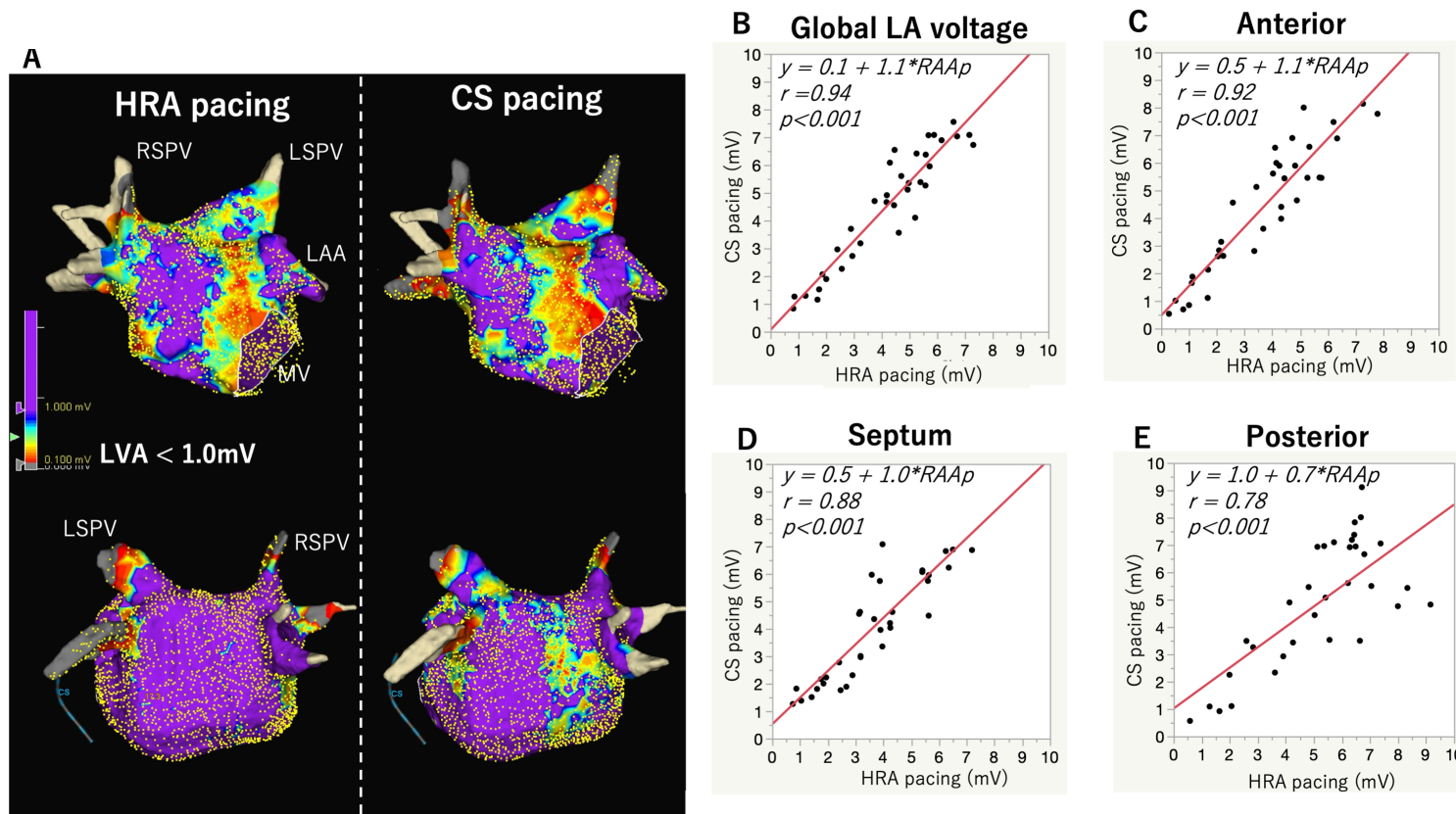
Figure S9. A, Comparison of V_{GLA} between GMC and CMC. There was a strong linear relationship between the two mapping catheters, and V_{GLA} by CMC

was 0.75 x V_{GLA} by GMC. B shows the 20-pole CMC with a 1-mm electrode length and 2-mm interelectrode spacing. CMC, circular mapping catheter; GMC,

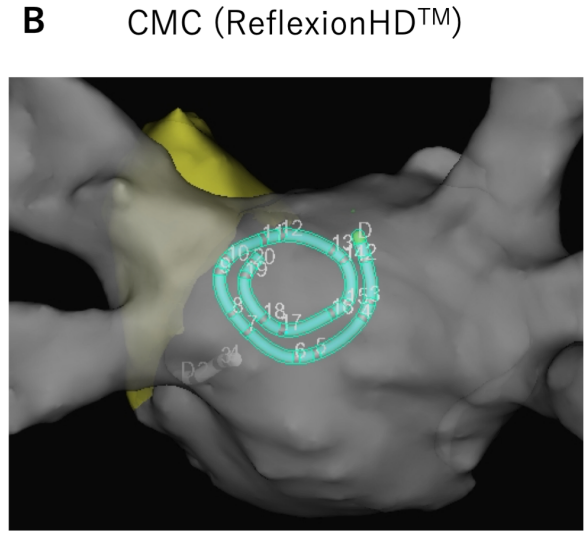grid mapping catheter; V_{GLA}, global LA voltage

A

$y = -0.2 + 0.75x$
$r = 0.979$
$P < 0.001$
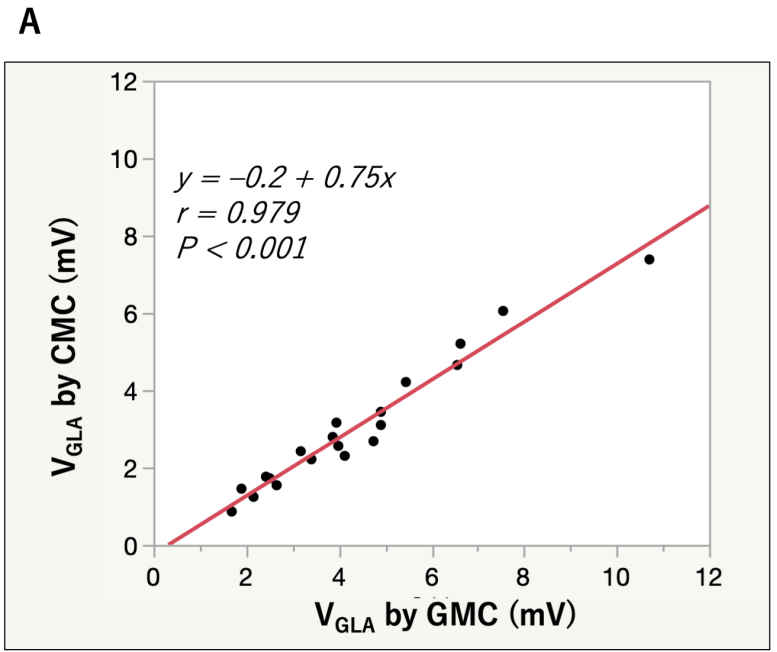
B   CMC (ReflexionHD™)

Figure S10. A, Representative cases of voltage map of the LA (upper row), activation map during left atrial (LA) macro-reentrant tachycardia (LAMRT, middle row), and ablation lesions at the critical isthmus (white arrows in lower row). The color gradient indicates serial changes in the electrogram amplitude from purple at ≥ 0.5 mV (voltage cutoff) to gray at <0.1 mV. Critical isthmuses were identified in the LVA. **B,** The inducibility of LAMRTs increased as the quartile moved down to the lower quartile. **C,** The inducibility increased as LVA appeared at lower voltage cutoffs. LAA, left atrial appendage; LSPV, left superior pulmonary vein; MV, mitral valve; RSPV, right superior pulmonary vein.
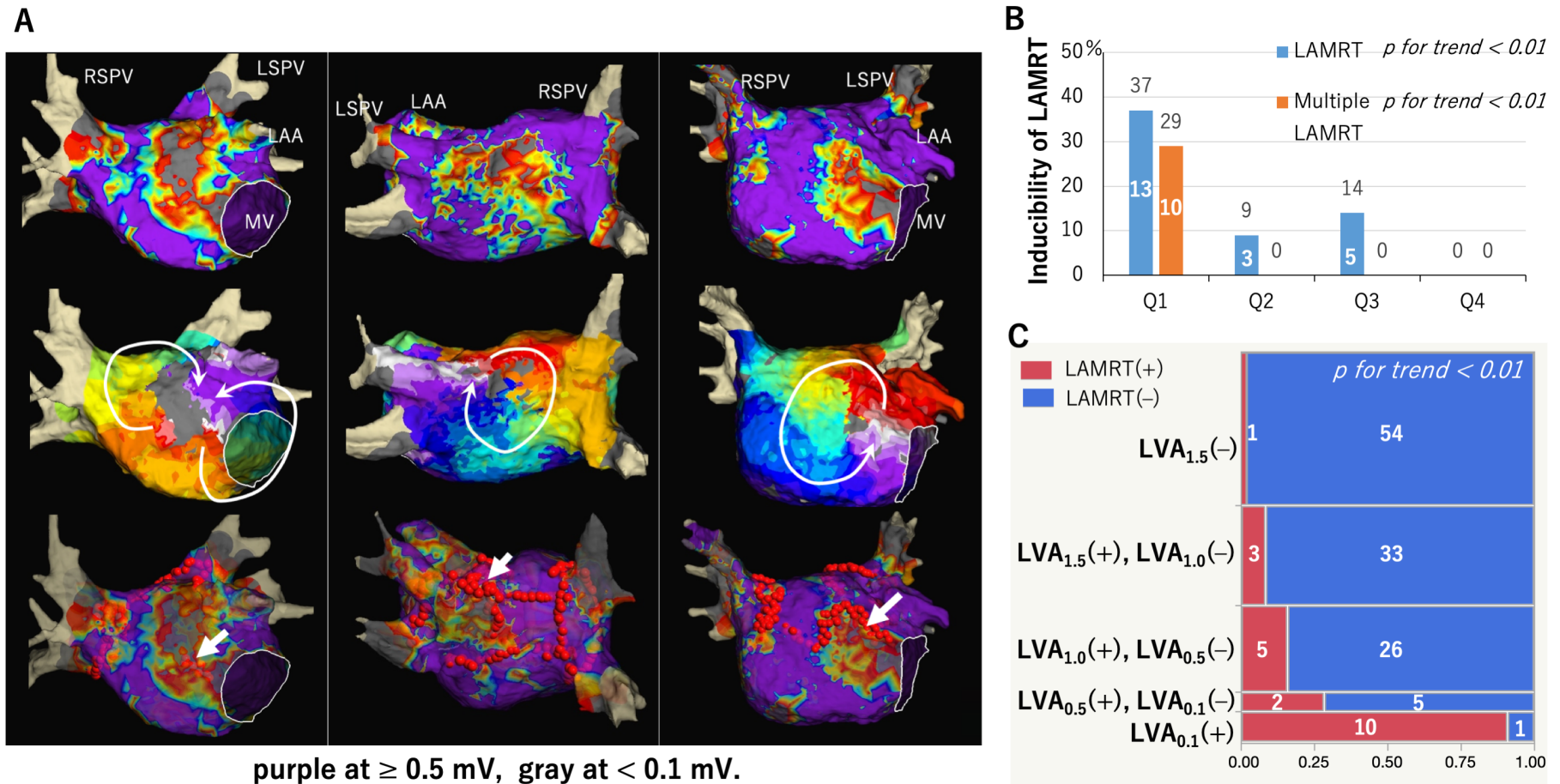

purple at ≥ 0.5 mV, gray at < 0.1 mV.

Figure S11. An example of voltage and activation map of the right atrial (RA) septum during high RA pacing. The locations of biopsy site at the limbus of fossa ovalis (FO) and FO were annotated on the geometry. Note that the voltage amplitude at the biopsy site is highest in the RA septum, showing > 11 mV in this case. No slow conduction zone was identified at the biopsy site. FO, fossa ovalis; IVC, inferior vena cava; TV, tricuspid valve; SVC, superior vena cava
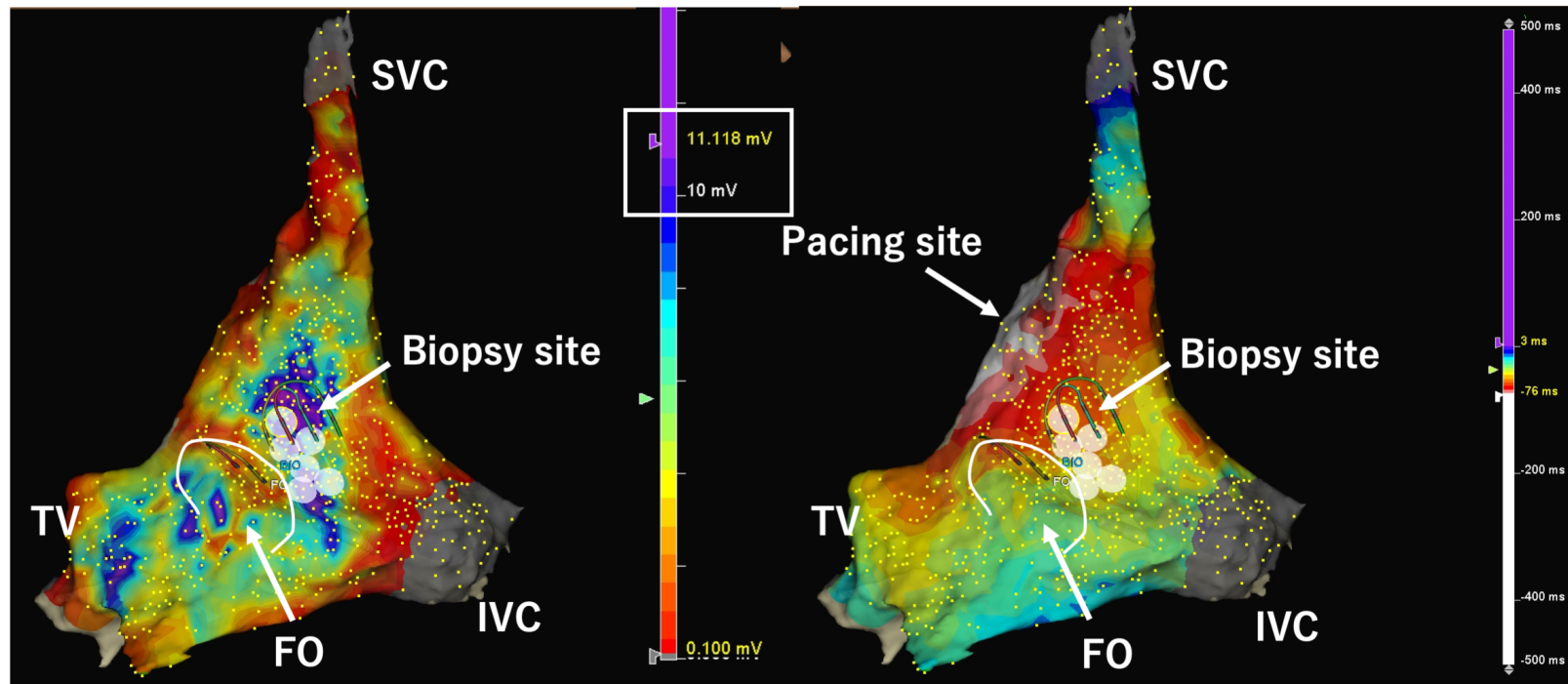
Figure S12. Relationship between V_{GLA} and V_{FO} and between V_{biopsy} and V_{FO}. There was a positive linear relationship between V_{GLA} and V_{FO}, and between

V_{biopsy} and V_{FO}. V_{biopsy}, voltage at biopsy site; V_{FO}, voltage at fossa ovalis; V_{GLA}, global LA voltage